THE EFFECT OF BENDING CYCLES ON OPTICAL AND ELECTRICAL PROPERTIES OF MULTILAYER ZTO/AG/ZTO AND ITO TRANSPARENT CONDUCTIVE OXIDE THIN FILMS GROWN BY MAGNETRON SPUTTERING

A Thesis Submitted to
the Graduate School of
İzmir Institute of Technology
in Partial Fulfillment of the Requirements for the Degree of

MASTER OF SCIENCE

in Physics

by
Cenkay ÇELİKLİ

October 2024
İZMİR

We approve the thesis of **Cenkay ÇELİKLİ**

Examining Committee Members:

Prof. Dr. Lütfi ÖZYÜZER
Department of Physics
Izmir Institute of Technology

Asst. Prof. Dr. Günnur GÜLER
Department of Physics
Izmir Institute of Technology

Prof. Dr. Mustafa EROL
Department of Physics Education
Dokuz Eylül University

17 October 2024

Prof. Dr. Lütfi ÖZYÜZER
Supervisor, Department of Physics,
Izmir Institute of Technology

Dr. Mehtap ÖZDEMİR
Co-supervisor,
TEKNOMA Technological Material Inc.

Prof. Dr. Lütfi ÖZYÜZER
Head of Physics Department

Prof. Dr. Mehtap Eanes
Dean of the Graduate School

ACKNOWLEDGEMENTS

First and foremost, I would like to express my heartfelt gratitude to my advisor and committee chair, Prof. Dr. Lütfi Özyüzer, for accepting me into his laboratory and providing me with the opportunity to work in the field of thin films. His guidance, support, and valuable contributions have played a significant role in my scientific development and the success of this thesis. I also wish to thank the other members of my thesis defense committee, Asst. Prof. Dr. Günnur GÜLER and Prof. Dr. Mustafa EROL, for insightful feedback and their valuable suggestions. I would like to express my heartfelt gratitude to Dr. Mehtap Özdemir for her invaluable contribution through her deep insights, constant support, and excellent guidance throughout various stages of my research.

Additionally, I would like to thank TEKNOMA Technological Materials Industrial and Trading Inc. for providing me with access to all the necessary infrastructure for my experimental work, along with their financial support throughout my thesis research.

And also I would like to thank Dr. Nursev Erdoğan, Seda Sürücü, and Aziz Taner Astarlıoğlu for their help and sharing ideas in this study. I would like to acknowledge the facilities of Research and Technology Centers, Turkish Aerospace (TUSAŞ). This work was supported by TUSAŞ with project number TM1001.

I would like to express my deepest gratitude to my mother Ayfer, my father Yıldırım, and my brother Berkay ÇELİKLİ, who have always encouraged, supported, and shown me endless love and understanding throughout my education. I feel incredibly fortunate to have such a wonderful family. I would like to thank my priceless wife Seval İkizoğlu and her family, who always inspire me to go further and support me by sharing their enlightening ideas. I would also like to thank our little sweet princess son Shaggy, who took me for walks frequently throughout my research process, who rested my mind while tiring my body, and who always made me happy with her cheerful jokes and loving looks.

I am also very grateful to my colleagues at Izmir Institute of Technology and my laboratory colleagues who are members of the ÖZYÜZER Research Group; first of all, Sıla Akar, Nesrin Yakar and Sinan Eroğlu, with whom I worked together, and later to Nurçin Karadeniz, Merve Ekmekçioğlu, Enver Deveci, Polatkan Özcan, Nazlıcan Esen,

Eray Ceyhan, Kübra Aras, Sanem Demirbaş, Musa Öztürk, Aileen Noori, Miray Akıncı, Muhammet Aydın, Hazar Birgül and Engin Baç, for sharing their vast knowledge with me and for their help.

I would like to thank my dear friends Yiğit Özkocaman and his wife İrem Şendinç, Burak Kaan Genç, Ece Kılıçlar, Gizem Taşkın, Emine Alaca and her husband Niyazi Kaşdan, Ecem Urçuk, Ezgi Uğur, Ece Ercan, who have always put me at ease by providing me with psychological support and therapy, and my friends in the automobile groups.

ABSTRACT

THE EFFECT OF BENDING CYCLES ON OPTICAL AND ELECTRICAL PROPERTIES OF MULTILAYER ZTO/AG/ZTO AND ITO TRANSPARENT CONDUCTIVE OXIDE THIN FILMS GROWN BY MAGNETRON SPUTTERING

This thesis aims to investigate and characterize the structural, electrical and optical properties of Zinc Tin Oxide (ZTO, Zn_2SnO_4)/Ag/ZTO (ZAZ) and Indium Tin Oxide (ITO, In_2O_3:SnO_2) thin films grown on flexible substrates before and after bending cycles.

There are many reasons why ITO and ZTO/Ag/ZTO (ZAZ) thin films were chosen for comparison. One of these main reasons is the decreasing availability of the Indium element in nature. Another reason is that the processing and market value of this element is relatively expensive. Due to these situations, researchers have started to search for new sources with higher availability and processability. As a result of the studies, a sandwich structure consisting of a Zinc Tin Oxide compound was developed as an alternative to the Tin doped Indium Oxide composition and the intermediate layer was completed using the Silver element. This structure offered similar properties to ITO in Transparent conducting oxide (TCO) materials requiring high conductivity and high transparency.

In experimental studies, optimum parameters were determined for thin film coated samples prepared using the magnetron sputtering technique and the necessary samples were prepared for characterization. In this process, after the substrates were prepared, the growth processes were completed, and the samples were made ready. The coatings were grown on polycarbonate (PC) rulers at room temperature. Adhesion test, profilometry and Scattering Electron Microscopy (SEM) were used for structural characterization of the samples, 2-probe and 4-probe methods were used for electrical characterization, and spectrophotometer was used for optical characterization.

As a result of this study, it was determined that the ZAZ multilayer structure performed better compared to ITO coatings. The obtained data revealed that an alternative ZAZ structure could be used to eliminate the use of ITO due to the limited availability of Indium. Additionally, this study not only demonstrates the potential of using ZAZ thin films instead of ITO thin films but also serves as a guide for the future applicability of ZAZ films in various flexible wearable material technologies.

ÖZET

BÜKÜLME DÖNGÜLERİNİN MIKNATISSAL SAÇTIRMA İLE BÜYÜTÜLMÜŞ ÇOK KATMANLI ZTO/AG/ZTO VE ITO ŞEFFAF İLETKEN OKSİT İNCE FİLMLERİN OPTİK VE ELEKTRİKSEL ÖZELLİKLERİ ÜZERİNDEKİ ETKİSİ

Bu tez çalışması, esnek alttaşlar üzerine büyütülen ZTO/Ag/ZTO ve ITO ince filmlerin, bükülme döngüleri uygulanmadan önce ve sonra yapısal, elektriksel ve optik özelliklerinin incelenmesini ve karakterizasyonunu amaçlamaktadır.

ITO ve ZAZ ince filmlerin kıyaslama için seçilmesinin bir çok sebebi vardır. Bu temel sebeplerden bir tanesi doğada İndiyum elementinin bulunabilirliğinin azalmasıdır. Bir başka sebep ise bu elementin işlenme ve piyasa değerinin görece pahalı olmasıdır. Bu durumlar nedeniyle araştırmacılar bulunabilirliği ve işlenebilirliği daha yüksek olan yeni kaynakların arayışına girmiştir. Çalışmalar sonucunda, Kalay katkılı İndiyum oksit bileşimine alternatif olarak, Çinko Kalay Oksit bileşiğinden oluşan sandviç yapı geliştirilmiş ve ara katman, Gümüş elementi kullanılarak tamamlanmıştır. Bu yapı yüksek iletkenlik ve yüksek şeffaflık gerektiren TCO malzemelerde ITO ile benzer özellikleri sunmuştur.

Deneysel çalışmalarda magnetron saçtırma tekniği kullanılarak hazırlanan ince film kaplı örnekler için optimum parametreler belirlenmiş ve karakterizasyon için gerekli örnekler hazırlanmıştır. Bu süreçte alttaşlar hazırlandıktan sonra büyütme işlemleri tamamlanmış ve örnekler hazır hale getirilmiştir. Kaplamalar oda sıcaklığında polikarbonat (PC) cetveller üzerine büyütülmüştür. Örneklerin yapısal karakterizasyonları için bant testi, profilometri ve Saçılma Elektron Mikroskobu (SEM), elektriksel karakterizasyonu için 2-prob ve 4-prob yöntemi, optik karakterizasyonu için spektrofotometre kullanılmıştır.

Bu çalışmada sonuç olarak, ZAZ çok katmanlı yapısının ITO kaplamalara kıyasla daha iyi performans gösterdiği belirlenmiştir. Elde edilen veriler, İndiyumun sınırlı olması nedeniyle ITO kullanımını ortadan kaldırabilecek alternatif bir ZAZ yapısının kullanılabileceğini ortaya koymuştur. Ayrıca bu çalışma sadece ITO ince filmler yerine ZAZ ince filmlerin kullanabilceğini göstermekle kalmayıp, gelecekte ZAZ filmlerin esnek giyilebilir malzeme teknolojisinde çeşitli uygulamalarda kullanilabilirliği açısından yol gösterir nitelik taşımaktadır.

TABLE OF CONTENTS

LIST OF FIGURES ix

LIST OF TABLES xi

CHAPTER 1 INTRODUCTION 12

1.1. The Purpose of This Thesis 16

CHAPTER 2 LITERATURE REVIEW 17

2.1. Optical and Electrical Properties of Silver Layer 17

2.2. Performance of Multilayer Structures 18

2.3. Mechanical Flexibility and Weathering Resilience 19

2.4. Comparative Studies and Future Directions 20

CHAPTER 3 EXPERIMENTAL DETAIL 23

3.1. Definition and Characteristics of Thin Films 23

3.2. Thickness Comparison 23

3.3. Deposition Techniques 24

3.3.1. Physical Deposition Methods (PDM) 25

3.3.2. Chemical Deposition Methods (CDM) 25

3.3.3. Solution-Based Chemistry 26

3.4. Magnetron Sputtering: Process and Mechanism 27

3.4.1. Process Mechanism 27

3.4.2. Role of Magnetic Field 28

3.5. Deposition Methods 29

3.5.1. Substrate Preparation 30

3.5.2. Film Deposition 30

3.5.2.1. ITO Film Deposition 30

3.5.2.2. ZTO Film Deposition 31

3.5.2.3. Ag Film Deposition 32

3.5.2.4. Au Film Deposition 32

3.6. Characterization Techniques of Films 33

3.6.1. Structural Characterization 33

3.6.2. Electrical Characterization 35
3.6.3. Optical Characterization 37
3.6.4. Electromagnetic Shielding 38

CHAPTER 4 RESULT 40
4.1. Structural Characterization 40
4.1.1. Adhesion Test 40
4.1.2. Thickness Measurements 40
4.1.3. SEM Analysis 41
4.2. Electrical Characterization 43
4.3. Optical Characterization 49
4.4. Electromagnetic Shielding 52

CHAPTER 5 CONCLUSION 56

REFERENCES 59

LIST OF FIGURES

Figure **Page**

Figure 1. Commonly used TCO materials and additional dopants in the literature, along with a comparison of the abundance of various materials. (Source: Pasquarelli et al., 2011) 13
Figure 2. The material structure type is defined by the energy band structure (Source: Ghorbani & Taherian, 2018) 15
Figure 3. Thin Film Thickness Range (Source: Sumarni Mansur, 2024) 24
Figure 4. Schematic representation of magnetron sputtering (Source: Hassan, 2017) ... 27
Figure 5. Schematic representation of coating layers on PC substrates 29
Figure 6. Image of film coated ruler substrates 29
Figure 7. Veeco DEKTAK 150 profilometer 34
Figure 8. KEITHLEY 2100 6 ½ Digit Multimeter 35
Figure 9. Experimental setup for measurements of ZTO/Ag/ZTO coated rulers Two probe method 35
Figure 10. KEITHLEY 220 Programmable Current Source 36
Figure 11. Experimental setup for measurements of ITO coated rulers Four probe method 37
Figure 12. Ruler substrate in the bending stage 37
Figure 13. UV/VIS/NIR Perkin Elmer Lambda 950 spectrophotometer 38
Figure 14. Samples during the tape test, a) ITO sample before tape removal, b) ITO sample after tape removal, c) ZAZ sample before tape removal, d) ZAZ sample after tape removal 40
Figure 15. Layer thicknesses of ZAZ and ITO coatings 41
Figure 16. SEM analysis of ZAZ as-grown thin films after 50 bending cycles, a) 300µm, b) 100µm, c) 50µm, d) 20µm scale image 42
Figure 17. SEM analysis of ITO as-grown thin films after 50 bending cycles, a) 300µm, b) 100µm, c) 50µm, d) 20µm scale image 42
Figure 18. SEM analysis of as-grown ITO thin films after 50 bending cycles using CBS after 50 bending cycle, a) 300µm, b) 50µm scale image 43
Figure 19. Resistance/Cycle graph of ITO 928-2 sample drawn with data obtained with 2-probe methods 44

Figure 20. Resistance/Cycle graph of ITO 928-4 sample drawn with data obtained with 2-probe methods 44
Figure 21. Resistance/Cycle graph of ITO 928-2 sample drawn with data obtained with 4-probe methods 45
Figure 22. Resistance/Cycle graph of ITO 928-4 sample drawn with data obtained with 4-probe methods 46
Figure 23. Resistance/Cycle comparison graph of ITO 928-2 and ITO 928-4 sample .. 46
Figure 24. Resistance/Cycle graph of ZAZ 192-3 sample drawn with data obtained with 2-probe methods 47
Figure 25. Resistance/Cycle graph of ZAZ 193-3 sample drawn with data obtained with 2-probe methods 47
Figure 26. Resistance/Cycle comparison graph of ZAZ 192-3 and ZAZ 193-3 sample 48
Figure 27. Comparative graph of normalized Resistance/Cycle of ZAZ192-3 and ITO 928-2 sample 48
Figure 28. Transmission graphs of the ITO 928-2 sample before and after the bending cycle 50
Figure 29. Transmission graphs of the ITO 928-4 sample before and after the bending cycle 50
Figure 30. Transmission graphs of the ZAZ 192-3 sample before and after the bending cycle 51
Figure 31. Transmission graphs of the ZAZ 193-3 sample before and after the bending cycle 51
Figure 32. S21 Transmission graph of LAITO928-2 sample 53
Figure 33. S21 Transmission graph of LAITO928-4 sample 53
Figure 34. S21 Transmission graph of T192-3 sample..... 54
Figure 35. S21 Transmission graph of T193-3 sample..... 54

LIST OF TABLES

Table **Page**

Table 1. The history of processes and creating TCOs (Source: Ginley, 2011) 14
Table 2. Thin film deposition methods and classification 24
Table 3. ITO thin film coating parameters 31
Table 4. ZTO thin film coating parameters 31
Table 5. Ag thin film coating parameters 32
Table 6. Au thin film coating parameters 32
Table 7. Layer thicknesses of ZAZ and ITO coatings 41
Table 8. Transmission values measured before and after the bending cycle 52

CHAPTER 1

INTRODUCTION

Transparent conducting oxides are electrical conducting materials that possess low light absorbing properties. TCOs are a class of materials that possess two key properties: Optical transparence, they transmit visible light through them and therefore they are considered as optically transparent. Electrical conductivity, even though they are rather transparent, they display good electrical conductivity, which is quite rare for most clear materials. TCOs were reported by Badeker when he first achieved the conducting property of CdO thin films prepared by sputtering cadmium in 1905 (Badeker 1907). These materials exhibit high optical transparency in the visible spectrum (Y. Zhu et al. 2006), allowing light to pass through with minimal absorption, and have good electrical conductivity, enabling the flow of electrical current while maintaining transparency. This property is essential for applications where both transparency and conductivity are required, such as in-touch screens, flat panel displays, electrochromic devices, and thin film solar cells. (Betz et al. 2006; Katayama 1999; Hosono 2007; Guillén and Herrero 2011; Granqvist 2007; Martin et al. 2004). They have low resistivity (Dhamodharan et al. 2015) which is essential for efficient conduction of electricity with minimal power loss. Also, they are chemically stable, resistant to oxidation, and can withstand exposure to harsh environments without significant degradation in performance (Mirletz et al. 2015).

Furthermore, TCO materials can be deposited as thin films on flexible substrates, making them suitable for applications requiring mechanical flexibility, such as flexible electronics and wearable devices (Guillén and Herrero 2011). It provides good contact and stability in device manufacturing due to its good adhesion properties to the substrates (H. Zhu et al. 2021). The ability to maintain its properties without deterioration at high temperatures encountered during the operation of the device is due to the good thermal stability of the TCO material. They can be tailored by adjusting the composition and deposition parameters, allowing for customization to meet specific application requirements (Chopra, Major, and Pandya 1983).

Some common TCO materials include Indium Tin Oxide. It is one of the most widely used TCO materials due to its high transparency in the visible region and good electrical conductivity. It is mostly used in applications such as flat panel displays (Ruske et al. 2007) touchscreens, and solar cells (Baxter and Aydil 2006), Zinc Oxide (ZnO) is another popular TCO material known for its high transparency and good electrical conductivity. It is used in including solar cells, light-emitting diodes and various optoelectronic devices (Lewis, 2000).

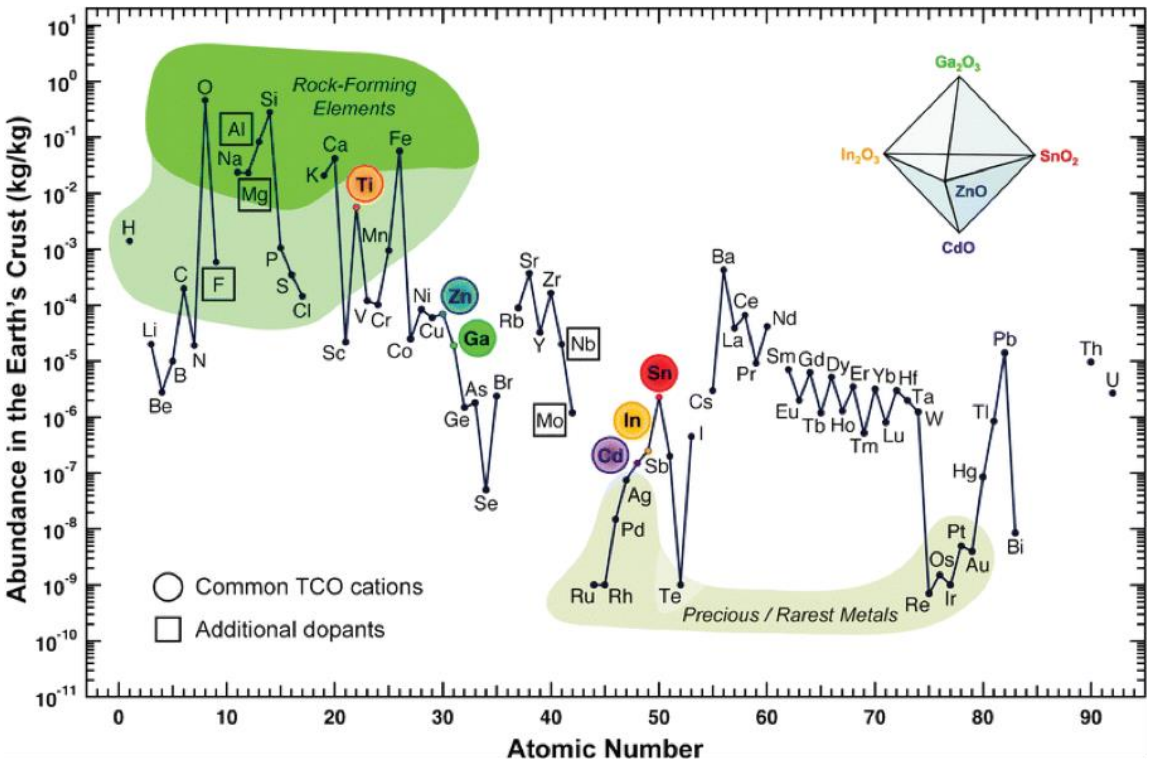

Figure 1. Commonly used TCO materials and additional dopants in the literature, along with a comparison of the abundance of various materials. (Source: Pasquarelli et al., 2011)

Doping is a common technique used to modify the properties of TCO materials as shown in Figure 1. Doping with elements like indium, gallium, aluminum, tin or fluorine can enhance the conductivity and transparency of TCOs (Heo et al. 2004; Singh, Chaudhary, and Pandya 2016) Fluorine-doped Tin Oxide (FTO) is another TCO material where tin oxide is doped with fluorine. In addition, Aluminium-doped Zinc Oxide (AZO) is another TCO material that offers high conductivity and good transparency (H. Zhu et al. 2014). It is often used as an alternative to ITO due to its lower cost and abundance of source materials. The need to obtain Zinc Tin Oxide stems from its unique properties and

advantages that make it valuable for various applications, especially in the field of TCOs. Alternative to Indium-Based TCOs because of indium scarcity and rising costs, the development of ZTO provides a cost-effective option for transparent and conductive coatings.

Table 1. The history of processes and creating TCOs (Source: Ginley, 2011)

Material	Year	Process	Reference
Cd-O			
CdO	1907	Thermally Oxidation	K. Badeker, Ann. Phys. (Leipzig) 22, 749 (1907)
Cd-O	1952	Sputtering	G. Helwig, Z. Physik, 132, 621 (1952)
Sn-O			
SnO_2:Cl	1947	Spray pyrolysis	H.A. McMaster, U.S. Patent 2,429,420
SnO_2:Sb	1947	Spray pyrolysis	J.M. Mochel, U.S. Patent 2,564,706
SnO_2:F	1951	Spray pyrolysis	W.O. Lytle and A.E. Junge
SnO_2:Sb	1967	CVD	H.F. Dates and J.K. Davis, USP 3,331,702
Zn-O			
ZnO:Al	1971		T. Hada, Thin Solid Films 7, 135 (1971)
In-O			
In_2O_3:Sn	1947		M.J. Zunick, U.S. Patent 2,516,663
In_2O_3:Sn	1951	Spray pyrolysis	J.M. Mochel, U.S. Patent 2,564,707 (1951)
In_2O_3:Sn	1955	Sputtering	L. Holland and G. Siddall, Vacuum III
In_2O_3:Sn	1966	Spray	R. Groth, Phys. Stat. Sol. 14, 69 (1969)
Ti-O			
TiO_2:Nb	2005	PLD	Furubayashi et al., Appl. Phys. Lett. 86, 252101 (2005)
Zn-Sn-O			
Zn_2SnO_4	1992	Sputtering	Enoki et al., Phys. Stat. Solid A 129, 181 (1992)
$ZnSnO_3$	1994	Sputtering	Minami et al., Jap. J. Appl. Phys. 2, 33, L1693 (1994)
a-ZnSnO	2004	Sputtering	Moriga et al., J. Vac. Sci. & Tech. A 22, 1705 (2004)
Cd-Sn-O			
Cd_2SnO_4	1974	Sputtering	A.J. Nozik, Phys. Rev. B, 6, 453 (1972)
a-CdSnO	1981	Sputtering	F.T.J. Smith and S.L. Lyu, J. Electrochem. Soc. 128, 1083 (1981)
In-Zn-O			
$Zn_2In_2O_5$	1995	Sputtering	Minami et al., Jap. J. Appl. Phys. P2 34, L971 (1995)
a-InZnO			
In-Ga-Zn-O			
$InGaZnO_4$	1995	Sintering	Orita et al., Jap. J. Appl. Phys. P2. 34, 1550 (1995)
a-InGaZnO	2001	PLD	Orita et al., Phil. Mag. B 81, 501 (2001)

ZTO (Zn_2SnO_4) has also advantages over ITO in terms of flexibility, thermal stability, better electrical performance, and compatibility with large-area deposition (Al Armouzi et al. 2021).

ZTO is often used in thin-film transistors (TFTs) and semiconductor applications due to its semiconducting properties, high electron mobility, and potential for use in electronic devices. ZTO is valued for its electrical properties rather than its transparency,

making it more suitable for applications where semiconducting behavior is required rather than transparent conductivity (H. Zhu et al. 2014).

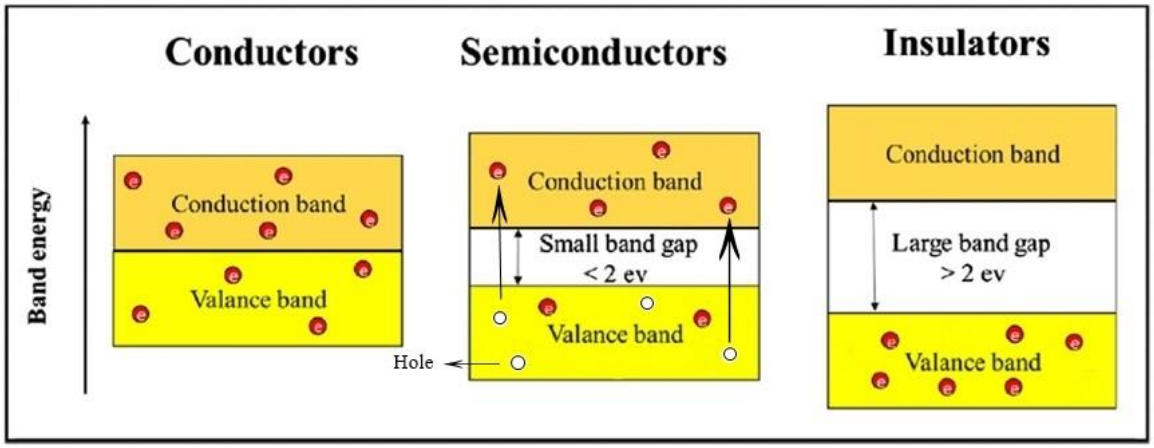

Figure 2. The material structure type is defined by the energy band structure (Source: Ghorbani & Taherian, 2018)

Since transparent conducting oxides are frequently induced by doping elements, they have high electrical conductivity and high optical transmission at specific 400–700 nm wavelengths. The most profitable oxide-based materials are n-type conductors with a large band gap oxide semi-conductor band gap of >3 eV. According to Lewis et al., TCO materials have an optical transmittance of about 80% in the visible region and weak electrical resistance of about 10^{-3}-10^{-4} Ω cm (Lewis 2000).

ZTO typically has a band gap in the range of 3.6 to 3.8 electron volts (eV) as a semiconductor material. The band gap of a material refers to the energy difference between the valence and the conduction band. This band gap value determines its optical and electrical properties. This property makes ZTO suitable for various high-energy applications (Dazai et al. 2020) ZTO structure combines with silver (Ag) to form ZTO/Ag/ZTO material and is used as multilayer coatings. So, each material has its strengths and applications within the TCO realm, with the ZTO/Ag/ZTO (ZAZ) multilayer structure offering a unique combination of properties for specific optoelectronic applications requiring both transparency and conductivity.

Studies show that the presence of Ag in the ZTO/Ag/ZTO (ZAZ) configuration potentially enhance the thin film performance of TCO applications as it maintains the electronic properties without losing its transparency (Kao, Chang, and Lin 2023; Dazai et al. 2020). For metal oxide materials, Behrendt et al. This was proven in experiments that

showed the added stability of the metal oxide layer through Sn-doping. Previous studies have also demonstrated that doping with oxygen atoms into the silver interstitial sites can lower the free energy of the silver mesh layer/oxidized phosphorus interface. This enhancement significantly improves dewetting capability and material stability while also impeding thermal degradation (Behrendt et al. 2015). Research on the stability of Oxide/Metal/Oxide materials subjected to high temperature and humidity conditions at 85°C / 85% reveals that SnO exhibits superior structural stability compared to other conductive metal oxides. Behrendt et al. experimentally approved that doping with Sn improves the stability of the metal oxide layer, as mentioned in the literature (Silva et al., 2023) On the other hand when it comes to the metal layer, Jeong et al.'s research results demonstrate that doping the oxygen atom interstitial sites with Silver(Ag) can lower the free energy of the interface for the silver middle layer, significantly enhancing dewetting and material stability while also hindering thermal degradation (E. Jeong et al. 2021).

1.1. The Purpose of This Thesis

In this thesis, direct current (DC) magnetron sputtering was used to create multilayer thin films of ZTO/Ag/ZTO over polycarbonate (PC) at room temperature for use in transparent conductive oxide (TCO) applications. The aim of this study is to growth, characterization, and after bending cycle structural, electrical and optical properties of ITO and ZTO thin films on polycarbonates.

While selecting these materials used in experimental studies, some important advantages were taken into consideration. ZAZ thin film optimized according to tin-doped indium oxide has been preferred, as it is abundant availability and also has low surface resistance, better performance, and less surface roughness.

As a result of the studies, the electrical and optical characterization of ITO and ZTO/Ag/ZTO coatings after the bending cycle process is presented in detail. In addition, it is envisaged that ZTO/Ag/ZTO multilayer films can be used as an alternative to ITO among TCO materials.

CHAPTER 2

LITERATURE REVIEW

In TCO/metal/TCO multilayer systems, the metal layers are frequently chosen based on the desired thin-film properties from different metals, such as molybdenum (Mo), copper (Cu), silver (Ag), and gold (Au). Three-layer structures such as ZTO/Ag/ZTO (Choi et al. 2011; Ekmekcioglu et al. 2021) and IZO/Au/IZO (J. A. Jeong, Park, and Kim 2010), ZnO/Ag/ZnO (Sarma and Sarma 2018; Sahu, Lin, and Huang 2006), AZO/Ag/AZO (Bingel et al. 2016; Jung et al. 2013; Sutthana, Hongsith, and Choopun 2010), NTO/Ag/NTO (Park et al. 2010) are reported for use in several applications. Since Ag thin films (< 20 nm thickness) display good transmittance in the range of 400-700 nm and low resistance, Ag is the most preferred middle layer in Dielectric / Metal / Dielectric multilayers. Various Dielectric / Ag / Dielectric multilayer films, including metal-based dielectrics like Sn (Shihui Yu et al. 2014), Ti-In-Zn, ZnS (Z. Yu et al. 2012), Al (Zhang et al. 2017), Zr (Song et al. 2013), Zn-Sn (Winkler et al. 2012), Zn (Mohamed 2008) and Ti (Wu et al. 2013) have been studied.

2.1. Optical and Electrical Properties of Silver Layer

According to previous research in the literature, Ag was chosen as the intermediate layer for the sandwich structure in this thesis study, and it was positioned between the ZTO layers. Studies, where Ag was used as the intermediate layer in multilayer materials and its optical and electrical properties, were compiled in the literature review that is given below. The bending process results (flexibility, resistivity, strength, etc.) were evaluated for various multilayer materials.

Wu et al. TiOx/Ag/TiOx (TAT) multilayers were constructed by amorphous TiOx films sandwiching an Ag layer of 10 to 25 nm in thickness, and detailed investigations of the optoelectrical characteristics were carried out by XRD, XPS, UV-Vis-NIR, and AFM, respectively. Their transmittance of the samples was < 88% at 550 nm. The best performance is obtained from the 18 nm film of the multi-layer sample among all the samples (Wu et al. 2013).

Moreover, Chiu et al demonstrated the ion-assisted deposition method used for electron-beam evaporation to create a transparent and conductive Ag layer sandwiched between two distinct TiO_2 and SiO_2 oxides. It was shown that 6.5 Ω/□ of sheet resistance and an average transmission of ~89% in the 400–700 nm wavelength range were acquired by optimizing the thicknesses of the dielectric films and metal (Chiu et al. 2014).

2.2. Performance of Multilayer Structures

In another study where Ag was used as a middle layer, Girtan examined the optoelectrical characteristics of ITO(20nm)/Ag(7nm)/ITO(20nm) that were sputtered onto PET and glass substrates using metallic targets such as In:Sn, Ag in an inert environment for metallic interlayers and a reactive atmosphere for oxides. At room temperature, the tri-layer films yielded a resistivity of around 3×10^{-5} Ωcm and a transmittance of ~90-97% at 550 nm (Girtan 2012).

To realize bulk-heterojunction organic solar cells, Choi et al. also focused on the optical and electrical properties of ZnO/Ag/MoO_3 multilayer electrodes which were prepared on glass substrates by radiofrequency and direct current sputtering, respectively. Even without a post-annealing treatment, the transparent composite electrodes showed a sheet resistance of 5 Ω/□, which was comparable to that of the ITO electrode of 20 Ω/□ (Choi et al. 2011).

Sarma et al. present a thorough investigation of transparent and conducting ZnO/Ag/ZnO thin films. ZAZ is deposited using the magnetron sputtering process on glass and flexible substrates. For ZnO/Ag/ZnO thin films deposited on glass substrates, the low sheet resistance of 17.0 Ω/□ and high transmission of 81.8% is obtained, while for ZnO/Ag/ZnO films grown on PET substrates, the low sheet resistance of 14.7 Ω/□ and high transmittance of 77,3% is noted. Understanding the effect of ZnO texture and residual stress on the electrooptical characteristics of ZnO/Ag/ZnO multilayer films is made easier by XRD research. XRD studies and electro-optical tests reveal that the main reason for the tensile residual stress of ZnO over a certain threshold, which is suitable for lower sheet resistance, is the lattice expansion in the cross direction to the film surface (Sarma and Sarma 2018).

2.3. Mechanical Flexibility and Weathering Resilience

In another study, using radiofrequency (RF) magnetron sputtering, transparent conductive zinc tin oxide (ZTO) thin films were grown on a glass. Sn-ZnO (ZTO) thin films were deposited on glass. The effect of spray powder (90-240 W) on the morphology, electrical, and optical properties of the samples was examined. According to the AFM pictures, ZTO films with minimal roughness (Rq) should be produced using low sputtering powers of less than 210 W. All the ZTO films had average light transmittances between 87.1 and 93.4% in the 400–900 nm wavelength range, although the light transmittance curves of the films deposited at high sputtering powers showed a multi-peak oscillation feature. The films' bandgaps showed a red shift in comparison to pristine ZnO, and they ranged from 3.18 to 3.31 eV (Shijin Yu et al. 2021).

The optical and electrical characteristics of highly conductive and transparent multilayer electrodes made by thermal evaporation of Ag and radiofrequency sputtering of tin-doped zinc oxide (ZTO) as the top connection point for transparent organic light-emitting diodes (TOLED) were examined by Winkler et al. At ~500 nm, ZTO/Ag/ZTO (20 nm)/(8 nm)/(39 nm) exhibited a transmittance of approximately 82% and a sheet resistance of 9 Ω/□ (Winkler et al. 2012).

In her master's thesis, Ekmekçioğlu is investigating the suitability of using ZTO as an anode instead of ITO thin film in OLED production. Initially, ZTO thin films were generated on soda lime glass using magnetron sputtering. Afterwards, flexible Polyethylene Terephthalate (PET) substrate was coated with ZTO thin film, and then Polyimide (PI) substrate was coated with ZAZ sandwich structured tri-layer thin film using the same magnetron sputtering technique. Spectrophotometry, energy-dispersive X-ray spectroscopy (EDS), scanning electron microscopy (SEM), X-ray diffraction (XRD), and Raman spectroscopy have all been used to examine the best coated thin films. The optimal parameters that were used were: DC power of 15 W; target-substrate distance of 7.0 cm; gas flow rate of 15.0 sccm Ar and 5.5 sccm O_2; deposition time of 10 min; and substrate temperature of 90.4 °C. These were the best conditions for optimizing the growth of ZnSnO thin films by ZT Target. As a result, a ZTO thin film thickness of 98.3 nm yielded sheet resistance and optical transmittance of 8.1 kΩ/□ and 90.1%, respectively. Additionally, it has been demonstrated that when ZTO thin film thickness increases, so does its sheet resistance. Consequently,

it is possible to reduce the upper layer of ZTO's sheet resistance. In this manner, optical transmission can rise while sheet resistance can be significantly reduced.

Subsequently, the ZAZ/Soda Lime Glass (SLG) multilayer thin film electrode was determined to have the lowest optical transmittance of 88.9% and the lowest sheet resistance of 12.6 Ω/□. Then, it was discovered that the ZAZ/PI multilayer thin film electrode had the lowest optical transmittance of 69.1% and the lowest sheet resistance of 13.0 Ω/□. Ultimately, it was discovered that the ZAZ/PET multilayer thin film electrode had the lowest optical transmittance of 62.0% and the lowest sheet resistance of 20.8 Ω/□ (Ekmekcioğlu, 2019).

2.4. Comparative Studies and Future Directions

Turkoglu's studies are similar to other studies, SLGs were used to create ZTO/Ag/ZTO electrodes at room temperature via DC magnetron sputtering. The effectiveness of these electrodes was examined in thin film thicknesses and the location of the Ag intermediate layer inside the multilayer. It was found that by varying the thicknesses of the top ZTO, middle Ag, and bottom ZTO films, it is possible to achieve lower sheet resistance and better optical transmittance. With a transmittance of 87.11% and a sheet resistance of 3.61 Ω/□, the highest FoM was 69.69×10^{-3} Ω^{-1}. When the manufactured multilayers' solar spectrum selectivity was examined, however, the multilayers with FoM ≤ 60.12×10^{-3} Ω^{-1} produced the best matches (Turkoglu et al. 2022).

Ekmekcioglu et al.'s research, for transparent conductive electrode (TCE) applications, ZTO/Ag/ZTO multilayer thin films were grown at room temperature using a direct current (DC) magnetron sputtering process on soda lime glass (SLG) and various polymer substrates, including polycarbonate (PC) and PET. Investigations were conducted into how the substrate affected the ZTO/Ag/ZTO multilayer films optical, structural, and electrical properties. ZTO/Ag/ZTO multilayer thin film grown on a 21 mm thick PC substrate at room temperature showed enhanced transmission due to higher absorption and lower reflection in the Ag thin film layer and decreased grain-boundary scattering. At 550 nm, the transmission of coated PET and PC is found to be 62% and 77%, respectively, while that of uncoated PET and PC is 58% and 75.9%. ZTO/Ag/ZTO electrodes can therefore be a good option for TCE applications due to their superior electrical and optical qualities (Ekmekcioglu et al. 2021).

Hengst et al. investigated the behavior of two and three layer coating systems which are composed of an electrode, an absorption layer, and a barrier for flexible a-Si:H solar cells under mechanical stress. Two sets of ITO conductive coatings were created to show how the microstructure of a single film influences the mechanical behavior of the entire multilayer coating. As layer thickness increased, the number of defects that cause crack formation increased along with the crack-starting strain of a-Si:H. It's interesting to note that as film thickness increased using roll-to-roll (R2R) sputtering, the crack onset strain (COS) of those films rose as well. This was explained by the films' growing compressive stress. Lastly, depending on the ITO film shape, the failure behavior of ITO/a-Si:H bilayers was investigated. Compared to ITO-2 and a-Si:H, the adhesion between ITO-1 and a-Si:H was shown to be (qualitatively) stronger (Hengst et al. 2017).

Kim and colleagues explored a new kind of flexible, transparent electrode made from a multilayer film composed of zinc tin oxide (ZTO), silver (Ag), and indium tin oxide (ITO). They tested these films on flexible PET (polyethylene terephthalate) substrates and found some impressive results. The ZTO/Ag/ITO films, with various layer thicknesses, showed a high level of transparency in the visible light spectrum, ranging from 79.4% to 89.2%. Notably, these multilayer films had lower electrical resistance compared to a standard ITO layer of the same thickness (60 nm). The study revealed that increasing the thickness of the silver layer from 6 nm to 14 nm led to a rise in both the carrier concentration and the mobility of the film. Specifically, the carrier concentration went up from 4.12x10^21 to 1.11x10^22 cm^3, and the mobility increased from 8.14 to 17.4 cm^2/Vs. The optimal configuration they found was a film with 20 nm of ZTO, 10 nm of silver, and 30 nm of ITO, which had a sheet resistivity of just 9 Ω/□. This combination also proved to be highly flexible, maintaining its performance even when bent. Overall, the research indicates that this ZTO/Ag/ITO multilayer film could be a great choice for flexible organic photovoltaic cells and photonic devices, thanks to its combination of transparency, low resistance, and flexibility. (Kim et al. 2015).

Seok et al. made a detailed comparison between the mechanical, electrical, and optical properties of RTR-sputtered ZTO/AgPdCu(APC)/ZTO thin films deposited on PET surfaces and those of conventional sputtered ITO films. In specifically, a lab-made bending, twisting, rolling, and folding test equipment was used to compare the mechanical flexibility of ITO and ZTO/APC/ZTO. The ZTO/APC/ZTO multilayer is effectively insulated against heat due to the low IR transmission and strong reflection of

the APC metal layer. Tests for bending, twisting, rolling, and folding verified the ZTO/APC/ZTO electrodes' exceptional mechanical flexibility (Seok et al. 2019).

In another work, Kao et al. conducted both outdoor and indoor accelerated weathering tests on commercial oxide/metal/oxide (abbreviated as OMO) samples made of ZTO/Ag/ZTO coatings on PET substrates. They investigated how environmental stressors like mechanical bending, high temperatures, and ultraviolet (UV) radiation affected the ways that OMO samples degraded. As a result, the OMO coatings' mechanical flexibility and bendability were reduced by the embrittled PET substrates. The study's findings offer a thorough grasp of the resilience and weatherability of flexible transparent conductive materials with an OMO based on silver (Kao et al., 2022).

For usage in affordable flexible organic solar cells (FOSCs), the mechanical flexibility of ZTO/Ag/ZTO tri-layer thin films coated on flexible PET substrates by roll-to-roll sputtering was examined by Lim et al. Using testing equipment for twist bending, stretching, and outer/inner bending created in laboratory conditions, the ZTO/Ag/ZTO films' resistance changed. It was demonstrated that the improved Ag layer (12 nm), positioned between two ZTO films, offered greater flexibility along with a low sheet resistance of 5.37 Ω/□ and a transmittance of 86.03%. When it came to outer bending durability, the ZTO/Ag/ZTO electrode outperformed inner bending. After cracks were generated, the overlapped films created a conducting channel, which was responsible for the variations between the crack initiation positions and the electrical resistance changes. The ZTO/Ag/ZTO electrode's resistance to 50,000 bending cycles was demonstrated by the outer bending fatigue test. Furthermore, the ZTO/Ag/ZTO multilayer's flexibility and ability to withstand an angle of up to 38° were demonstrated by the twisting test. Compared to the traditional ITO film, the uniaxial stretching test demonstrated superior stretchability, with cracks beginning at 3% strain. This suggests that the transparent and flexible R2R sputtered ZTO/Ag/ZTO tri-layer electrodes are a potentially reasonable electrode choice in cost-sensitive applications of FOSCs (Lim et al. 2012).

Experimental methods based on the literature studies cited above will be explained in detail in Chapter 3.

CHAPTER 3

EXPERIMENTAL DETAIL

3. Thin Films and Deposition Techniques

3.1. Definition and Characteristics of Thin Films

Thin films are coatings made on surfaces or substrates by using one or the other established deposition methods. These films could be classified as 2D materials based on the assertion of thin films being very thin and having a thickness that is significantly lower than other layers (Tvarozek et al. 1998). The employment of thin films in this technology gives it a relatively high surface-to-volume ratio, which makes them different from bulky materials with the same composition (Mylvaganam et al. 2014). Generally, thin films are thin layers with a thickness of fewer than one micrometer, usually on the order of tens of nanometers.

3.2. Thickness Comparison

According to Figure 1, thin films are intermediate range regarding their thickness as they are not physically as thin as materials that have a thickness of the atomic or molecular scale but are thinner in comparison to sheets/plates. For instance, foil may be thinner than thin films but not as thin as any layer of material that may perhaps be termed thick films the thickness of which is more than 1 μm.

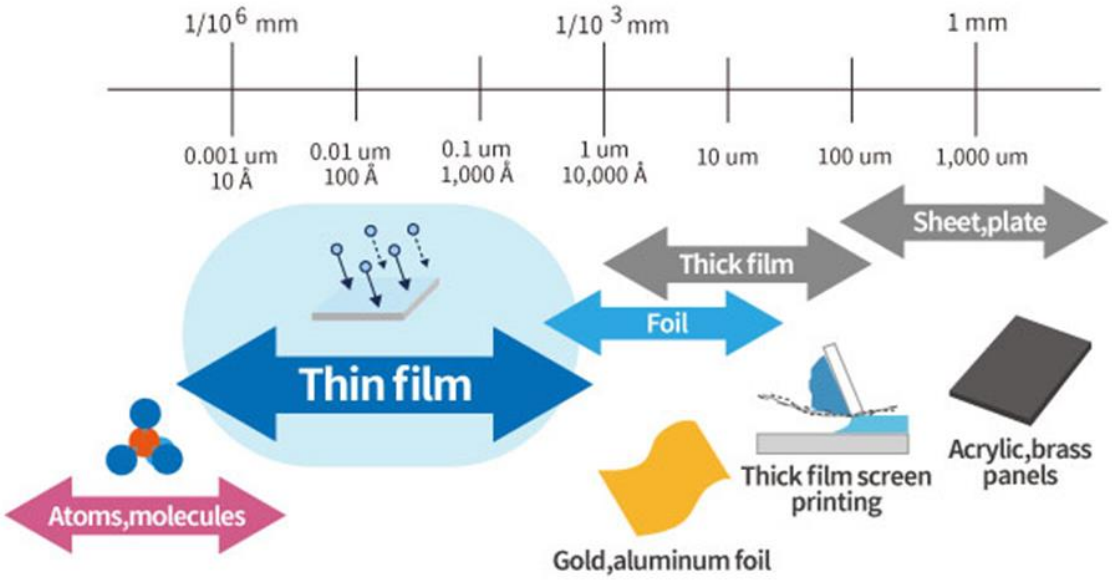

Figure 3. Thin Film Thickness Range (Source: Sumarni Mansur, 2024)

3.3. Deposition Techniques

Table 2. Thin film deposition methods and classification

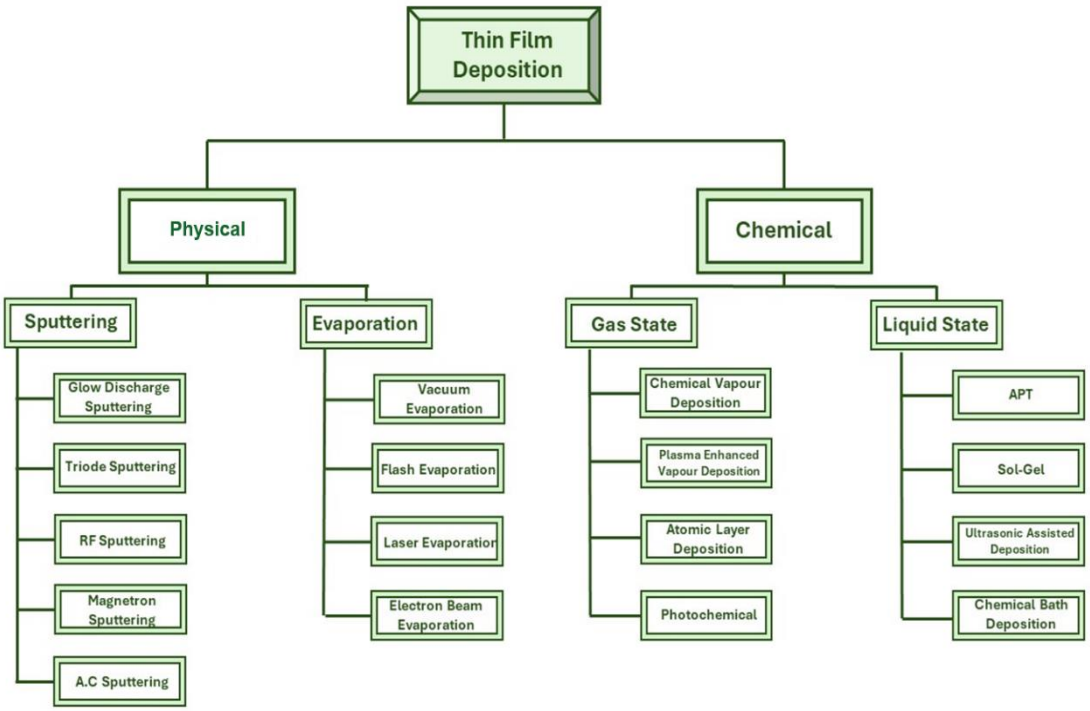

Thin film deposition methods are essential techniques used to create thin coatings on various substrates. There are a few different ways to deposit thin films, and they can be grouped into three main types: Physical Deposition Methods (PDM), Chemical Deposition Methods (CDM), and Solution-Based Chemistry. These methods are commonly employed in fields such as semiconductors, optics, and energy systems. Each method offers distinct advantages and is suited for different applications and materials. Together, these techniques play a critical role in modern technology and materials science.

3.3.1. Physical Deposition Methods (PDM)

Physical deposition methods are vacuum-based method used for thin film coating processes. In this technique, a solid or liquid material is vaporized and then condensed onto a substrate to form a thin film. The PVD process consists of three main stages: the vaporization of the material, the transport of the vapor through the vacuum chamber, and the condensation of the vapor onto the substrate.

Common PVD techniques include thermal evaporation, which is suitable for materials with low melting points, sputtering, which uses plasma to eject atoms from a target material, and molecular beam epitaxy (MBE), which allows for precise control of film properties.

The advantages of PVD include high purity, excellent adhesion, and a wide range of applicable materials. This method has significant applications in the production of electronic components, optical coatings, decorative finishes, and enhancing the durability of cutting tools. Overall, PVD plays a critical role in modern materials science and engineering.

The Magnetron Sputtering method, which is a PVD techniques and is also used in this thesis, is examined in detail under the heading 3.4.

3.3.2. Chemical Deposition Methods (CDM)

Chemical deposition methods are techniques used to create thin films or coatings on substrates through chemical reactions. Chemical vapor deposition techniques, also known as CVD, involve using high temperatures. What happens is that the precursor is

heated up until it turns into a gas. Then, this hot gas is reacted with the surface of the substrate, which leads to the formation of a thin film.

Among these methods, Chemical Vapor Deposition (CVD) involves the reaction of gaseous precursors to form solid films on heated substrates, making it ideal for applications in semiconductors and protective coatings. Atomic Layer Deposition (ALD) is a specialized form of CVD that deposits films one atomic layer at a time, allowing for precise control over thickness, which is particularly valuable in semiconductor manufacturing.

The sol-gel process transitions a liquid sol into a solid gel, leading to thin film formation after drying and annealing, and is commonly used for ceramics and optical devices. Electrochemical deposition utilizes electric current to reduce metal ions from a solution onto a substrate, finding applications in electroplating and battery manufacturing. Lastly, the Langmuir-Blodgett technique allows for the controlled deposition of monolayers of surfactant molecules onto substrates.

Overall, these methods offer advantages such as uniformity, versatility in materials, and precise control over film properties.

3.3.3. Solution-Based Chemistry

Solution-based chemistry involves chemical reactions that occur in a liquid phase, typically with solutes dissolved in a solvent. In this category, chemical solutions can be used to make different kinds of films. Thick films, thin films, multilayered films, porous films, and dense films can be created (Ukoba et al., 2018). Key concepts include solubility, concentration, and reaction conditions, which influence reaction rates and outcomes.

Common techniques include precipitation reactions, solvothermal and hydrothermal synthesis, the sol-gel process for creating thin films, and electrochemical methods for driving reactions.

The advantages of this approach are its versatility, scalability for industrial use, and the ability to control reaction conditions effectively. Applications of solution-based chemistry are vast, including the synthesis of nanomaterials, drug formulation, and environmental chemistry for assessing water quality.

In my thesis, films were grown using the magnetron sputtering method, which is a physical deposition method. To understand this study, it is necessary to examine this method in detail.

3.4. Magnetron Sputtering: Process and Mechanism

Magnetron sputtering is one of the deposition techniques that falls under physical vapor deposition otherwise referred to as PVD and is used widely in thin film applications. It encompasses phenomena in which atoms are ejected from a target and then deposited on a substrate. This technique is appreciated due to high-rate deposition thickness with very good uniform thin films.

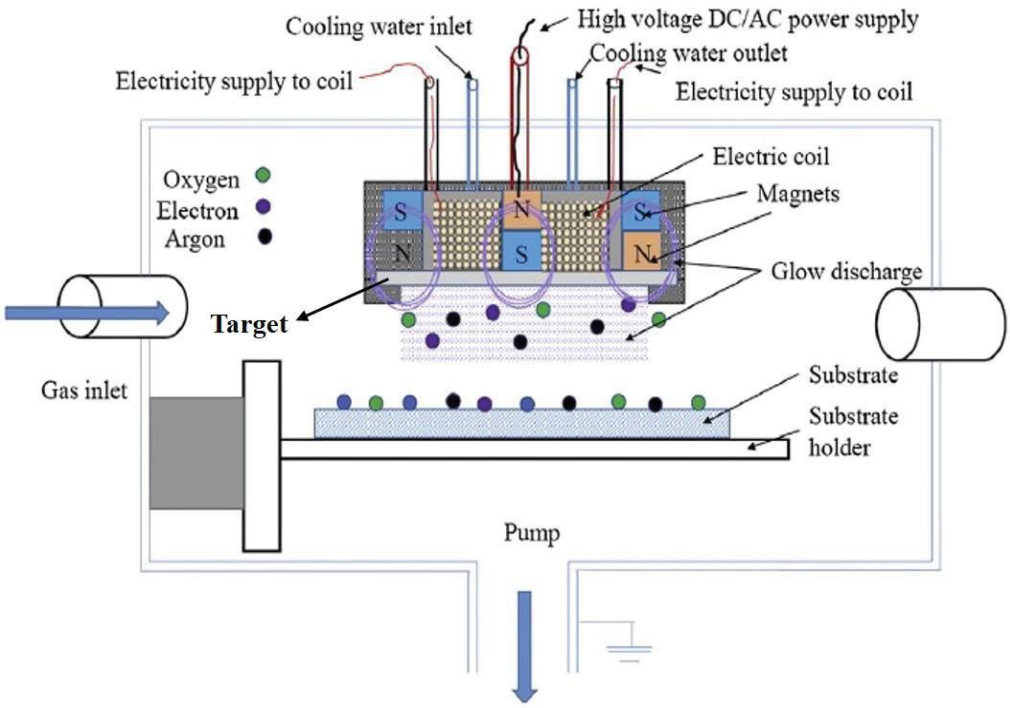

Figure 4. Schematic representation of magnetron sputtering (Source: Hassan, 2017)

3.4.1. Process Mechanism

Ionization of Argon Gas: The appropriate noble gas such as argon gas is introduced into the vacuum chamber. This is because already the anode is at a higher

potential as compared to the cathode which makes it ionize the Argon gas and Argon gas transforms to Argon ions (Ar+).

Acceleration of Ions: The ionized argon particles are then attracted or repelled by magnets within the Sputter gun towards the target material depending on the applied electric field, which is a function of the potential difference between the two electrodes.

Collision with Target Material: The argon ions that get ionized reach high kinetic energies and collide with the target material atoms. When it interacts with a target material, a portion of the energy with which Argon ions are traveling is felt by the atoms in the particular material. This energy transfer makes the atoms in the target material to be ejected out of the surface. It is also characterized by a sequential process in which material is expelled from the target to the substrate which is known as sputtering.

Deposition on Substrate: The atoms emitted by the target material pass through the vacuum and in turn condense on the substrate to produce a layer of thin layer.

3.4.2. Role of Magnetic Field

Magnet Configuration: On top of these magnets target material resides whereas at the other end of the magnets, a magnetic field is applied to the target material. This magnetic field is important in confining the plasma in the surrounding of the target material surface.

Efficiency Enhancement: The applied electric field ensures that the electrons are kept nearest to the target material, which in turn increases the frequency of ionization of argon gas. It also creates a higher presentation of ions within the confined area hence presenting a dense ionization which implies that there are more Argon ions which in an instance can hit the target material hard enough to sputter it. The argon ions are directed to the target material through the influence of a magnetic field to improve the rapture and abraded of the material.

Magnetron sputtering is one of the most effective processes in thin film deposition prospecting on the ionization of Argon gas and application of magnetic field for improved sputtering. Hence, with the feeble regulation of the thin-film deposition process and properties of the target material, high-quality thin films can be sputtered and deposited on different substrates for uses in electronics, optics, and even material science.

3.5. Deposition Methods

In my study, ZTO/Ag/ZTO (ZAZ) and ITO thin film layers were grown on polycarbonate (PC) rulers using the magnetron sputtering technique to observe the effect of the bending process on the thin film properties. Additionally, experimental studies on transparent conductive oxide materials such as AZO, ITO, and ZTO, utilizing this technique, have also contributed to the literature (Turkoglu et al. 2018; Ozbay et al. 2020; Ekmekcioglu et al. 2021). Subsequently, before proceeding with the multilayer film growth process, the parameters (coating power, pressure, gas ratios, etc.) for depositing the ZTO thin film layer were examined and optimized. In our study, the layers of the thin films are shown in Figure 5, and the final state of the samples placed on the sample holder used for coating these films is shown in Figure 6.

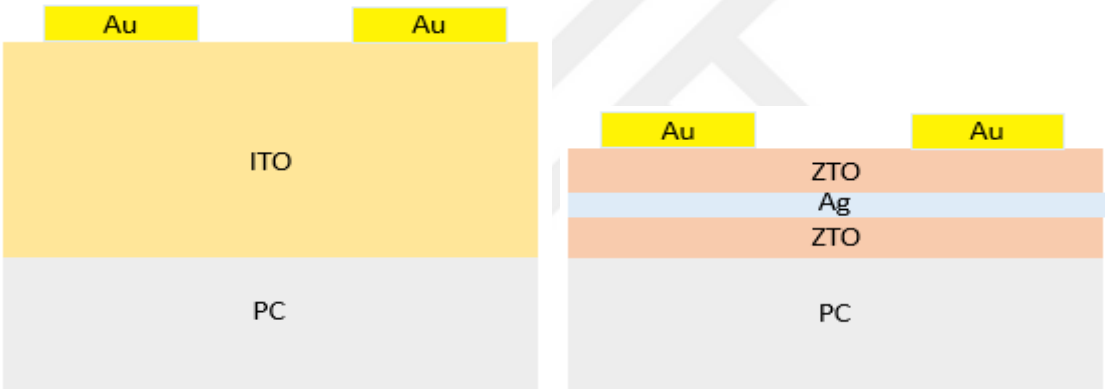

Figure 5. Schematic representation of coating layers on PC substrates

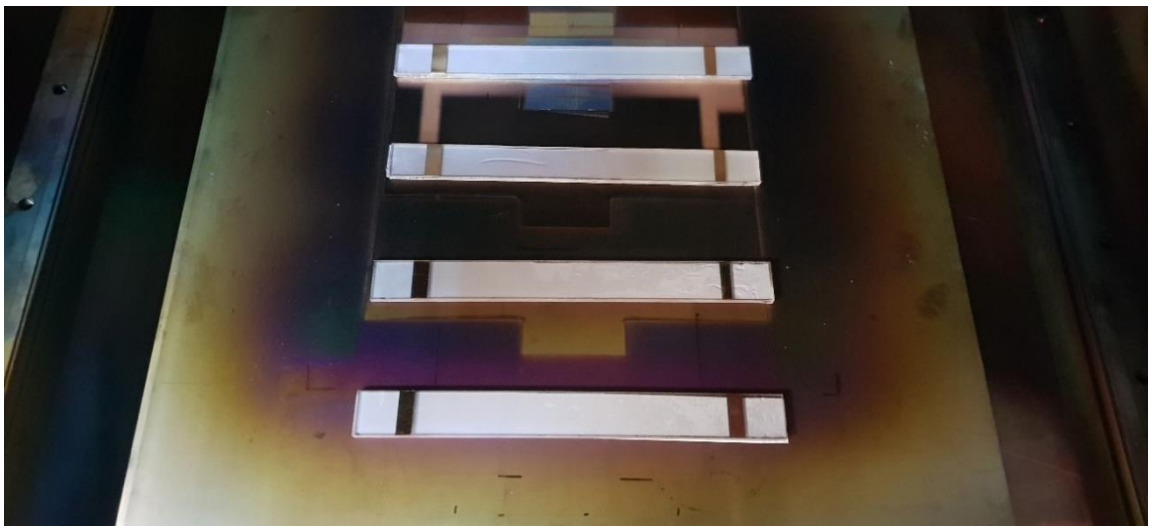

Figure 6. Image of film coated ruler substrates

This system entails two 2-inch magnetron sputtering sources, water cooling, and controlling gas inlet and electrical power supply. To obtain the high vacuum region of 1.0x10-5 hPa was done using both a turbo molecular pump (TMP) and a mechanical pump. The pressure of the system was monitored with the help of a full range vacuum gauge. At the pressure of 1.0x10-5 hPa, a mass flow controller was used to control the flow rates of 137 sccm Argon (Ar) gas (high purity 99%). The operating pressure after the gas was sent was measured using a baratron and plasma was produced inside the chamber by using a DC power supply.

3.5.1. Substrate Preparation

In my thesis, to examine the coating properties, flexible and durable Polycarbonate (PC) ($C_{16}H_{14}O_3$) material in large sizes was cut into 30x3x0.6 cm dimensions and prepared in the form of a ruler. Before the ZTO/Ag/ZTO films were grown, the protective layers on the PC samples were removed and cleaned using C_3H_8O Propanol with ≥ 99.0% purity and placed in the system. Later, a Gold (Au) contact layer was coated on the ITO and ZAZ coatings for electrical characterization. These stages will be examined under the headings.

3.5.2. Film Deposition

Under this heading, the parameters of the ITO, ZTO, Ag and Au coatings made in the thesis study are given in detail under separate headings.

3.5.2.1. ITO Film Deposition

To make a comparative analysis of the ZAZ coatings, the ITO coatings deposited in the in-line system which the moving substrate holder were enlarged with the following parameters. Besides, there are other parameters which include the following; when the system reached down to $6.0x10^{-7}$ Torr pressure, Ar (80.0 sccm) and O_2 gas (2.5 sccm) were sent, and the target sample distance was kept at 7.5 cm and the substrate holder speed is set to 9 cm/min.

Table 3. ITO thin film coating parameters

Sample	Power (W)	Voltage (V)	Current (A)	Working Pressure (mTorr)
LAITO-928	900	370	2.46	2.23

3.5.2.2. ZTO Film Deposition

To achieve the objectives of this study, such as good optical transmittance and low sheet resistance, we developed the growth of ZTO/Ag/ZTO tri-layer thin film electrodes in a sandwich structure as follows. In fact, in the current study, several layers with the lowest sheet resistance were formed by depositing silver as an interlayer on the films using the magnetron sputtering process.

In addition to these parameters, in this 150 cm diameter cylindrical system which moving targets, the optimum speed of the target (10 cm/min) was determined as a result of previous studies, and the speed of the target was kept the same in coating. The same amount of Ar gas (137 sccm) was sent to the system in during coating and the distance between the target and the sample was set as 8 cm.

Table 4. ZTO thin film coating parameters

Sample	Power (W)	Voltage (V)	Current (A)	Working Pressure (mTorr)
T-192-1	77.88	354	0.22	7.76
T-192-2	80.08	364	0.22	7.82
T-192-3	79.42	361	0.22	7.84
T-193-1	76.56	348	0.22	7.70
T-193-2	77.22	351	0.22	7.71
T-193-3	77.66	353	0.22	7.74

3.5.2.3. Ag Film Deposition

The Ag layer selected as the mid layer of the ZTO/Ag/ZTO film in the sandwich structure was completed with the following parameters in each coating. In addition to these parameters, 137 sccm Ar gas was sent to the system throughout the coating and the target sample was passed from 10 cm to scan at 80 cm/min.

Table 5. Ag thin film coating parameters

Sample	Power (W)	Voltage (V)	Current (A)	Working Pressure (mTorr)
T-192	48.45	323	0.15	7.76
T-193	48.00	320	0.15	7.69

3.5.2.4. Au Film Deposition

To examine the electrical properties of ITO and ZAZ coatings, a 10 mm wide Gold (Au) contact layer was coated on both ends of the samples, with the target at a height of 7 cm and scanning the sample at 9 cm/min, with the parameters given in the table below. As in other layers, 137 sccm Ar gas was sent to the chamber in this layer. The coated contact layer is shown in Figure 6.

Table 6. Au thin film coating parameters

Sample	Power (W)	Voltage (V)	Current (A)	Working Pressure (mTorr)
Au	45.73	412	0.11	7.89

In order to precisely characterize the ITO coated ruler samples, which will be examined in detail under the section 4.2. Electrical Characterization, and to eliminate the contact resistance formed in the 2-probe method, two more Au contacts were coated symmetrically with the same parameters.

3.6. Characterization Techniques of Films

Many methods can be employed in the characterization of thin films about the material quality. Structural properties of thin films are achieved through SEM analysis and thickness measurements. Characterization of the electrical properties of the materials is done by the two-point and four-point measurements. The optical properties of films are investigated with the transmission measurements. This section aimed to describe various experimental techniques and instrumentation for the applications leading to the characterization of the properties of the ZTO and ITO thin film.

3.6.1. Structural Characterization

Adhesion testing on thin films is performed to evaluate how well the film adheres to a substrate. This test is critical in many areas such as electronic components and optical applications. Tape testing is a common method used to evaluate the adhesion quality of thin films. Then, the adhesive tape is carefully placed on the film and quickly removed. The amount of film remaining on the tape and the condition on the surface are observed. These results are used to determine the durability of the material and potential needs for improvement.

A profilometer is a surface contact that has a stylus that is scanned systematically over the sample to measure the thickness of a layer. From the data that is obtained through scanning of the surface a three-dimensional height profile is reconstructed. In the drawing, the stylus can react to nuances of the direction of the upright surface. To measure the thickness of a thin film photoresist was dripped onto the substrate prescribed the following procedure: Subsequently, to enhance the contrast between the film and the substrate after the deposition of the former, the layer of the photoresist was removed using acetone.

The thickness measurements of the ZTO/Ag/ZTO and ITO thin films were determined using a Veeco DEKTAK 150 surface profilometer.

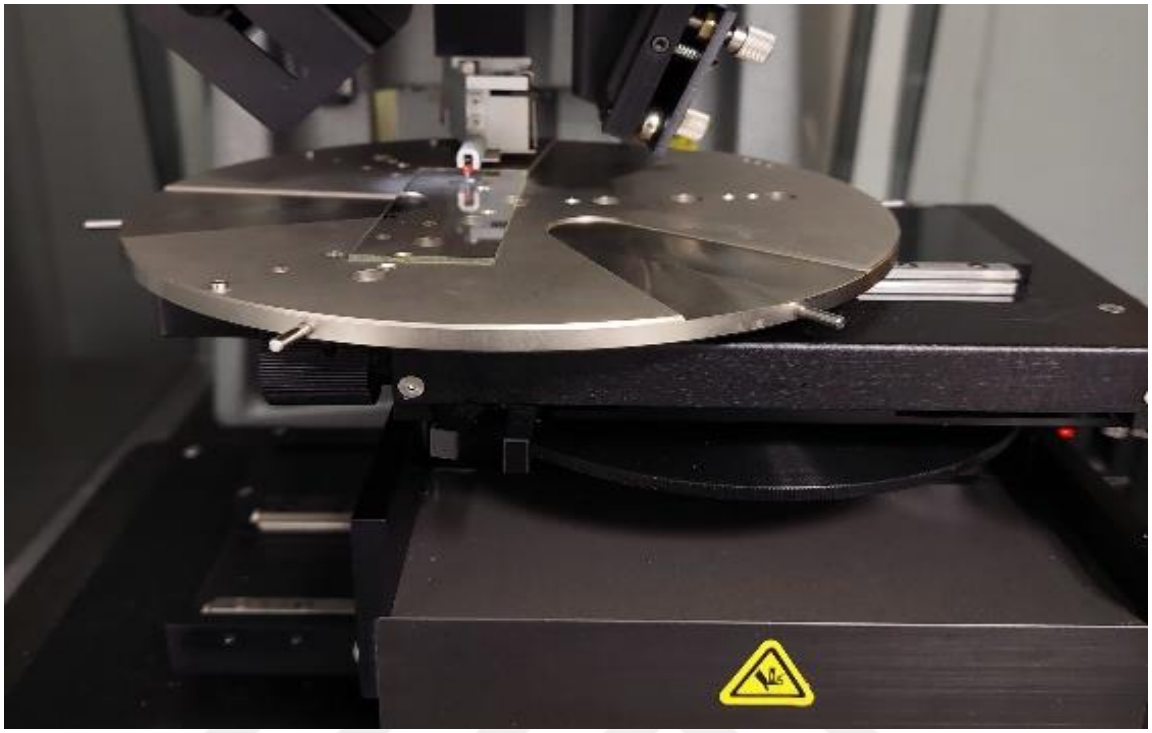

Figure 7. Veeco DEKTAK 150 profilometer

Scanning Electron Microscopy (SEM) is a highly effective tool for analysing the surface structure and composition of materials at very high magnifications. SEM works by directing a beam of electrons onto the sample's surface. The interaction between the beam and the surface atoms causes electrons to be either emitted or ejected, producing secondary electrons, backscattered electrons, and X-rays. The secondary and backscattered electrons are then collected to create detailed images of the sample, including topographical and elemental maps. This technique allows us to see very fine surface details and analyse the material's microstructure with precision.

In this thesis, the surfaces of the selected thin-film deposited samples were analyzed using the FEI-Quanta FEG 250, a high-performance SEM equipped with a field emission gun. The surface topography was imaged using a Circular Backscatter Detector (CBS) and an accelerating voltage of 7 kV at 10,000X magnification in a high vacuum with a spot size of 4.0.

3.6.2. Electrical Characterization

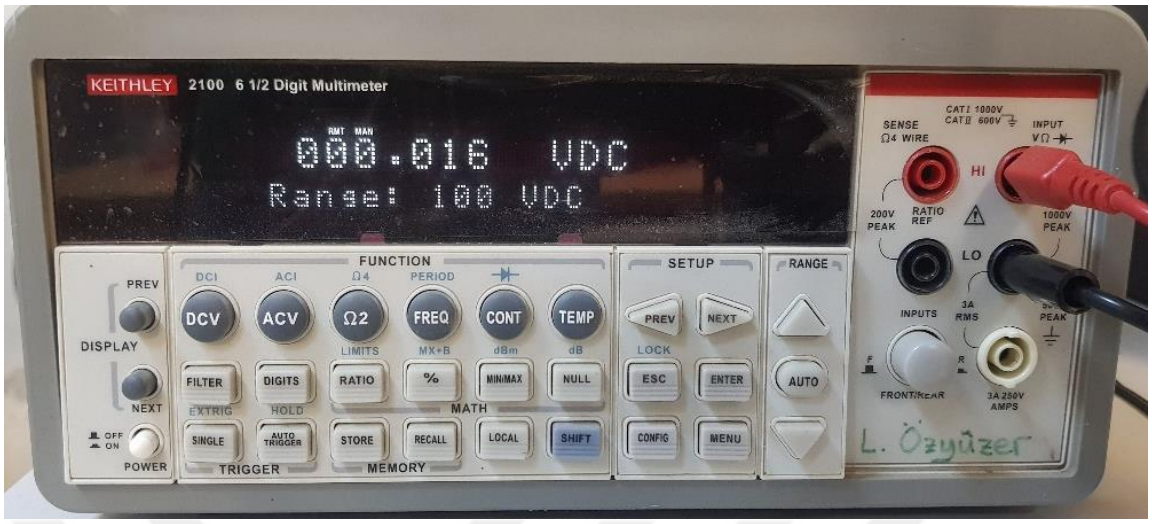

Figure 8. KEITHLEY 2100 6 ½ Digit Multimeter

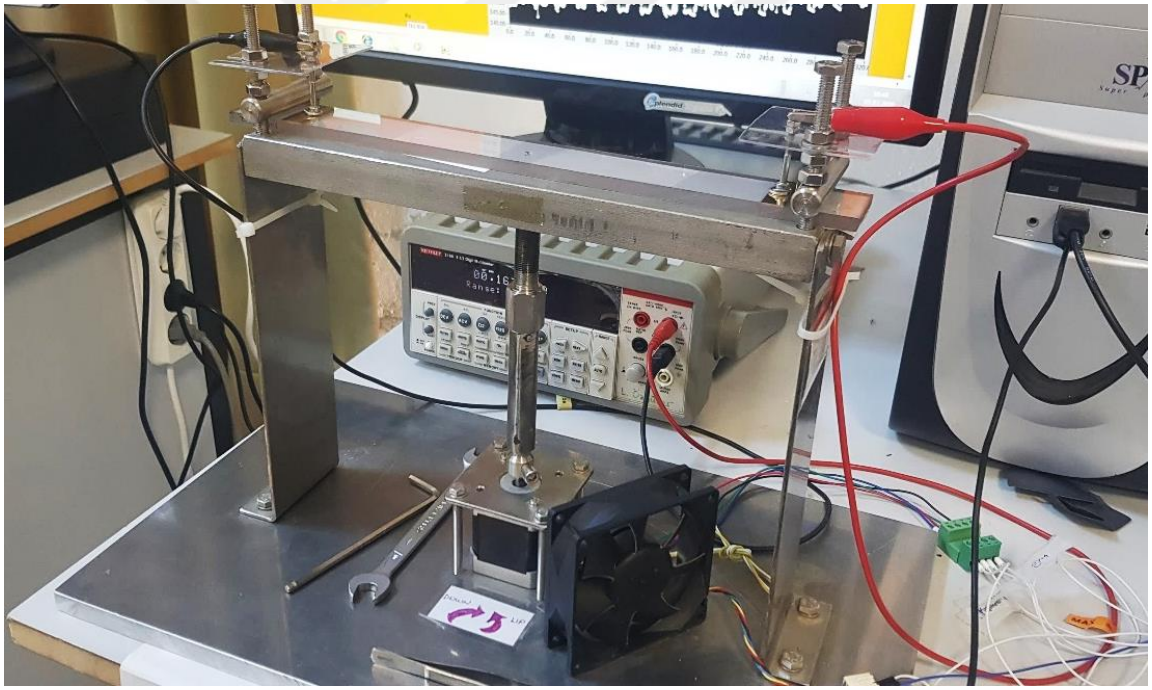

Figure 9. Experimental setup for measurements of ZTO/Ag/ZTO coated rulers Two probe method

The electrical properties of deposited ZTO/Ag/ZTO and ITO thin films were extensively studied. The measured resistance value was taken from the system KEITHLEY 2100 6 ½ Digit Multimeter while the bending process measurements were

taken on every increment of 0.025 mm. Data were recorded by making 50 complete cycles for each sample.

As a result of the tests performed on ITO thin film coated rulers, it was stated that four gold contacts were coated using the 4-probe method in order to obtain more sensitive measurements and eliminate contact resistance under the heading 3.5.2.4. Au Film Deposition. The current source required for the method used in the electrical characterization of the ITO rulers was selected as KEITHLEY 220 Programmable Current Source and 1.0mA constant current (3V max voltage) was applied and the resistance values were recorded via the KEITHLEY Digit Multimeter.

In Figure 10, Figure 11 and Figure 12, the current source used for characterization, the experimental setup and the visuals of the sample in the testing process are presented respectively.

Figure 10. KEITHLEY 220 Programmable Current Source

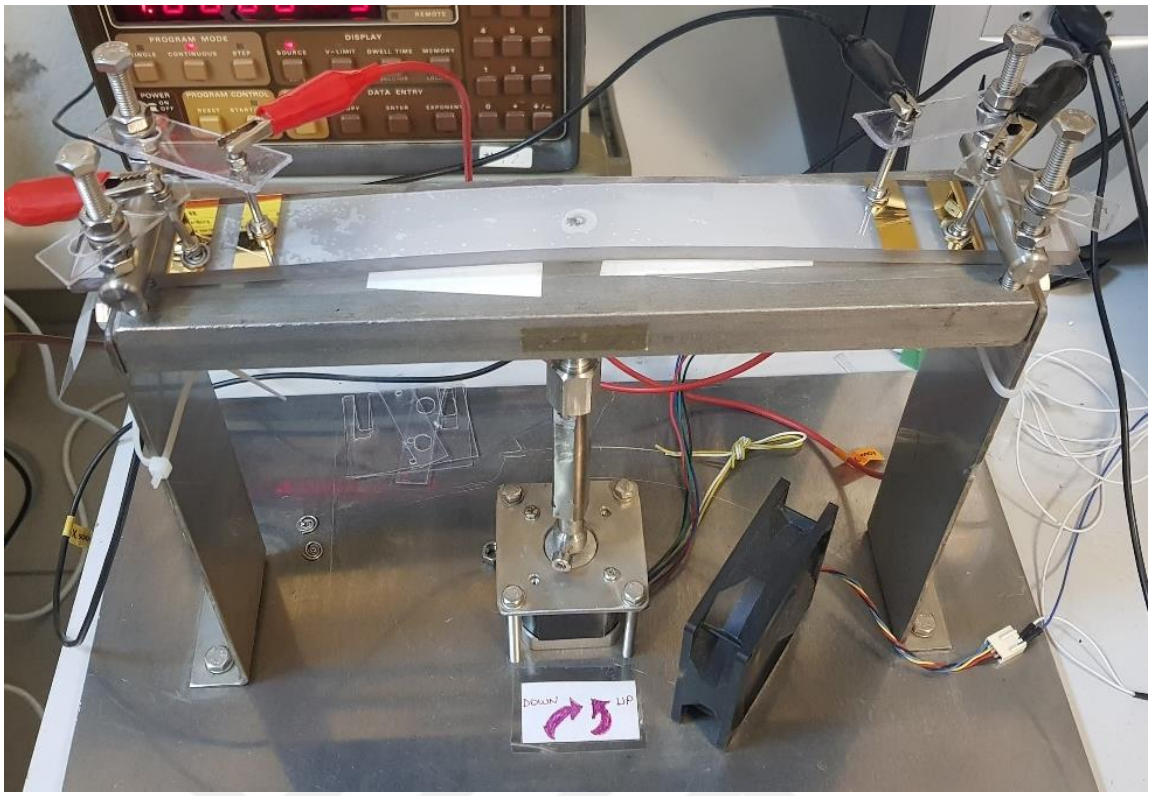

Figure 11. Experimental setup for measurements of ITO coated rulers Four probe method

Figure 12. Ruler substrate in the bending stage

3.6.3. Optical Characterization

The coated samples were characterized for their optical properties with the help of UV/VIS/NIR Perkin Elmer Lambda 950 spectrophotometer, where the optical

transmission of the synthesized films was carried out in the wavelength region 200-2600 nm.

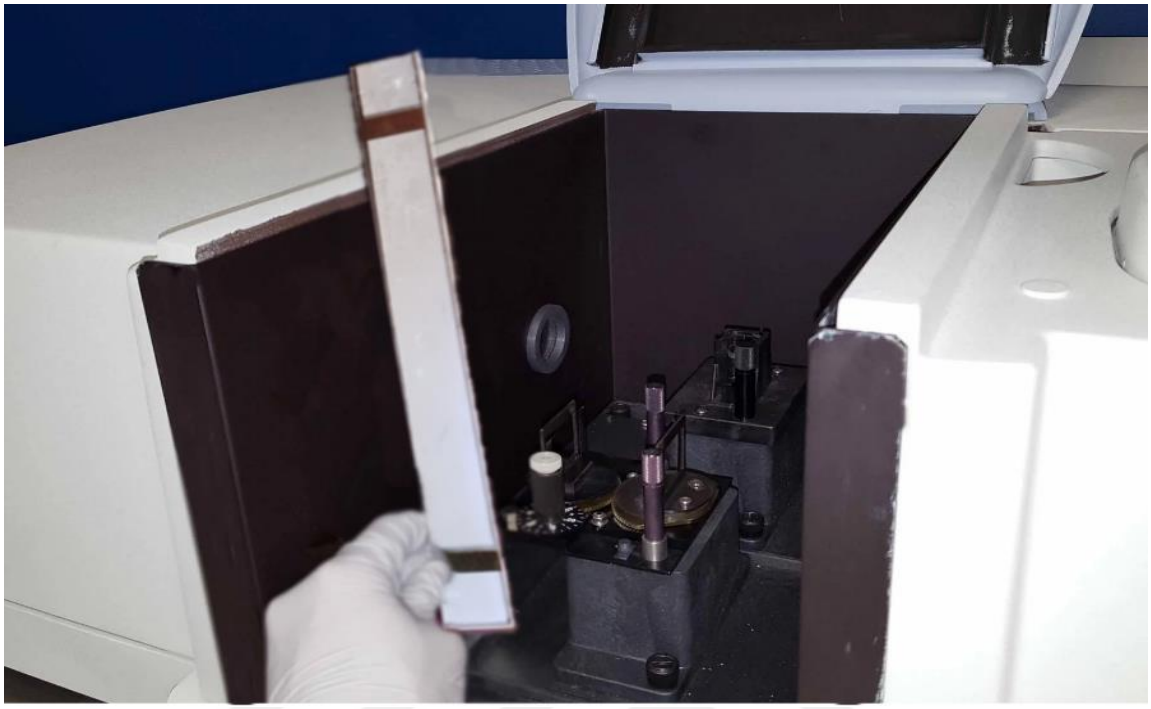

Figure 13. UV/VIS/NIR Perkin Elmer Lambda 950 spectrophotometer

3.6.4. Electromagnetic Shielding

The electromagnetic testing method uses electricity and magnetism in the detection and assessment of faults, fractures, corrosion, or other conditions of materials. The strategy here adopted is that magnetic fields and electric currents (or either of them) are produced within the test FRP composite while the electromagnetic signal is measured. Some of the identified EM techniques are; Eddy current (EC) inspection, Microwave open-ended waveguide imaging, Couple spiral inductors, alternating current field measurement (ACFM), magnetic flux leakage (MFL), and remote field testing (RFT). They all develop different physics based on their, own partial differential equations (PDEs).

Let's use the formula for attenuation or power change in dB:

$$A_{dB} = 10 \log\left(\frac{P_{out}}{P_{in}}\right)$$

If *P*out (output power) is less than *P*in (input power), the ratio will be less than 1, and the logarithm of a fraction (less than 1) is negative.

For instance, if the output power is only 1/10th of the input power, the attenuation would be:

$$A_{dB} = 10\log_{10}\left(\frac{1}{10}\right) = 10(-1) = -10dB$$

This means the wave has lost 10 dB of power, or 90% of its original power has been attenuated, leaving only 10% of the initial power.

In electromagnetic shielding, a negative dB value would describe how much EM energy is reduced after passing through a shield. For instance, a -20 dB shielding effectiveness means that only 1/100th of the EM wave's original power gets through the shield.

In this study, S21 transmission measurement was performed using Agilent 8720ES S-parameter Network Analyzer, 50 MHz to 20 GHz, with WR90 waveguide in the frequency range of 8.20 GHz and 12.40 GHz. The discussion of the data obtained is under the title 4.4. Electromagnetic Shielding is presented.

CHAPTER 4

RESULT

4.1. Structural Characterization

4.1.1. Adhesion Test

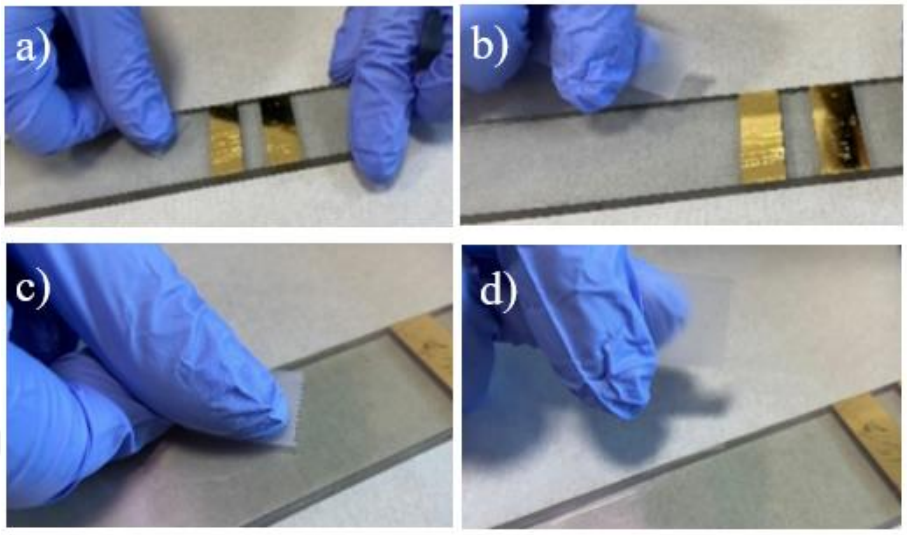

Figure 14. Samples during the tape test, a) ITO sample before tape removal, b) ITO sample after tape removal, c) ZAZ sample before tape removal, d) ZAZ sample after tape removal

The adhesion strength of thin film-coated samples was assessed using the tape test method. Figure 14 illustrates the adhesion strengths of both ITO and ZAZ coated samples on a PC substrate. The results indicated that neither film detached from the surface nor exhibited breakage upon tape removal, suggesting that the adhesion quality and strength were considerably high.

4.1.2. Thickness Measurements

The thicknesses of the growth processes, which were made to be the same as the optimum values determined as a result of previous studies for structural characterization,

were determined using the Veeco DEKTAK 150 surface profilometer. Thickness measurements were determined by scanning the region where the photoresist layer was removed from the substrate and the region where the film was grown.

As a result of the measurements, the thickness of the ITO coatings was measured as 247 nm, the layers of the ZTO/Ag/ZTO coatings were measured as 34 nm/15 nm/35 nm, respectively, and the thickness of the Au layers used for electrical measurements was measured as 69 nm.

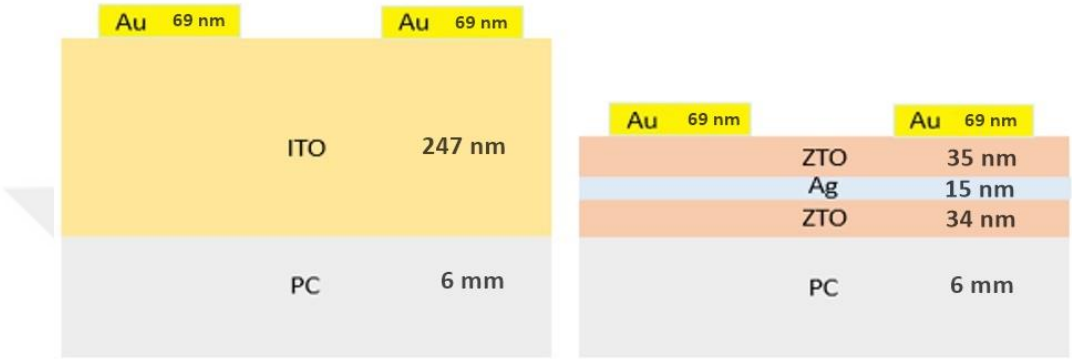

Figure 15. Layer thicknesses of ZAZ and ITO coatings

Table 7. Layer thicknesses of ZAZ and ITO coatings

	ZAZ				ITO	
Layer	**Bottom**	**Middle**	**Top**	**Au**	**First**	**Au**
Thickness (nm)	34	15	35	69	247	69

4.1.3. SEM Analysis

Figure 16 shows the SEM images of the ZAZ grown ruler samples after 50 bending cycles at 300µm, 100µm, 50µm and 20µm scales, respectively. Figure 16 shows the same-scale SEM images of the ITO grown rule samples after 50 bending cycles.

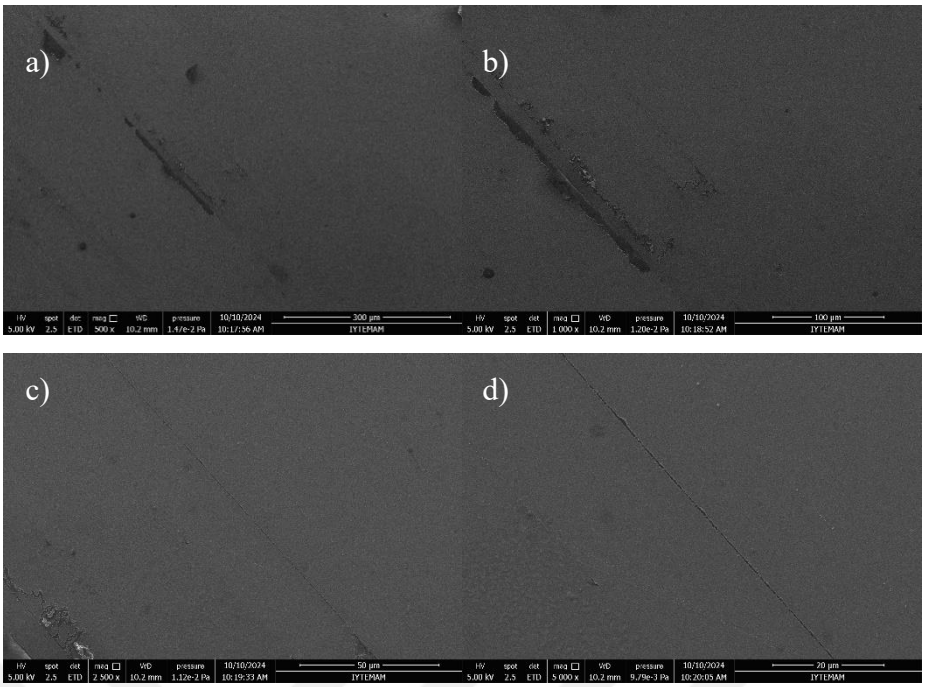

Figure 16. SEM analysis of ZAZ as-grown thin films after 50 bending cycles, a) 300µm, b) 100µm, c) 50µm, d) 20µm scale image

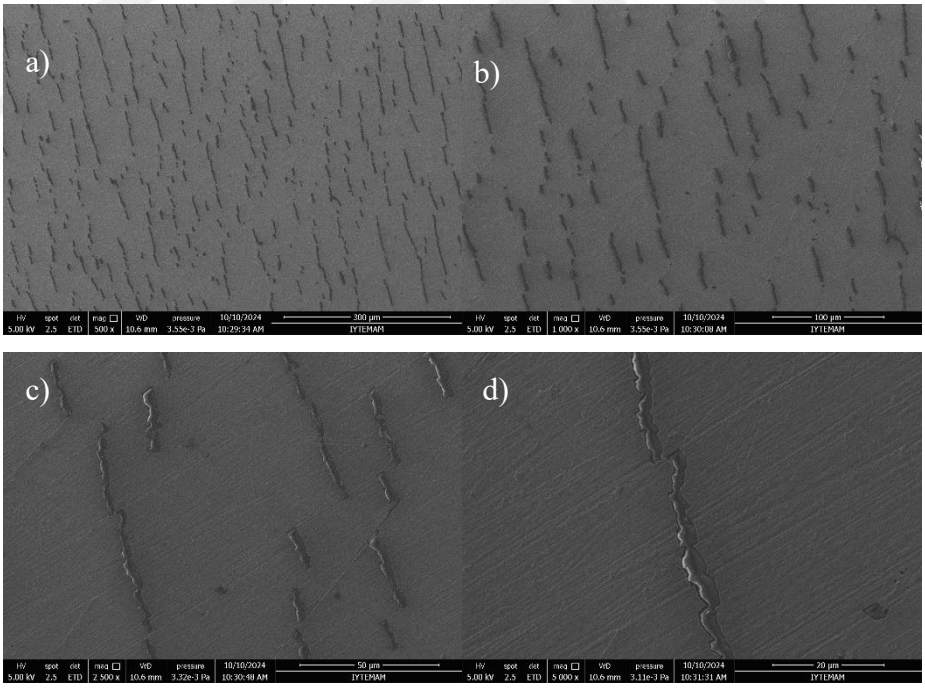

Figure 17. SEM analysis of ITO as-grown thin films after 50 bending cycles, a) 300µm, b) 100µm, c) 50µm, d) 20µm scale image

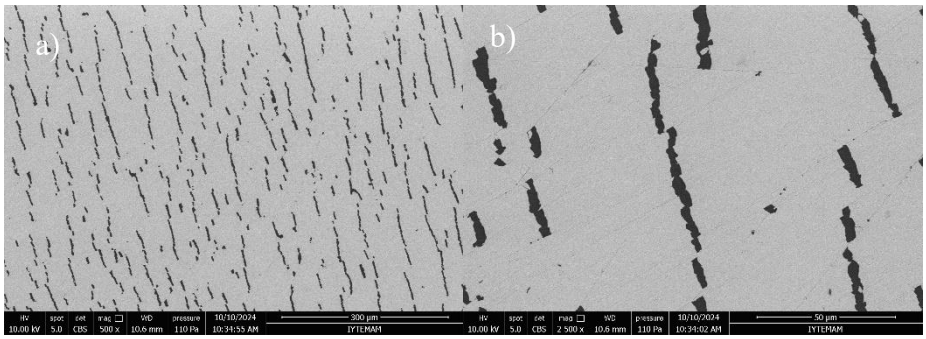

Figure 18. SEM analysis of as-grown ITO thin films after 50 bending cycles using CBS after 50 bending cycle, a) 300µm, b) 50µm scale image

Figure 18 shows the detailed surface topography of the ITO samples using CBS-Z Contrast and the SEM images are shown. Here Z is expressed as atomic number. In the CBS images, high atomic number samples are bright and low atomic number samples are dark. Dark cracks represent Carbon atoms (low atomic number) in the substrate, and bright areas represent Indium (ITO, high atomic number) atoms. After the tests, more cracks were observed on the ITO-coated samples than on the ZAZ-coated samples. This result explains the irregularities in the graph seen in Figure 27.

4.2. Electrical Characterization

When the electrical characterization of ZAZ and ITO coated rulers was performed during the bending process using the coating parameters presented in the experimental section, the following graphs were obtained and discussed.

Figures 19 and 20 show the Resistance/Cycle graphs drawn with the data obtained with the 2-probe method for ITO samples.

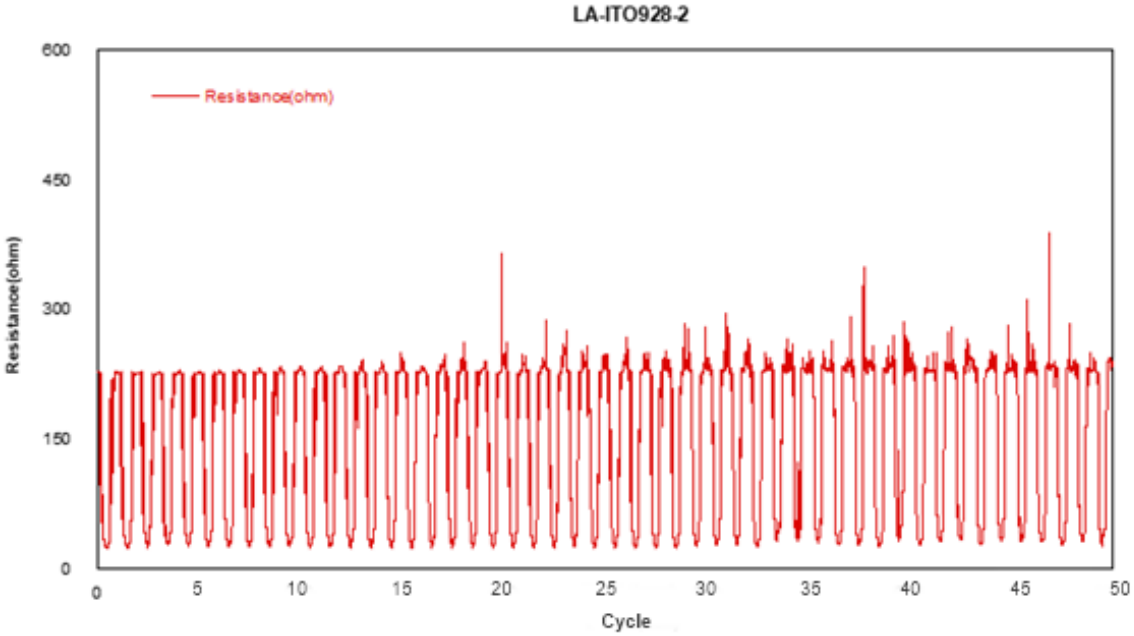

Figure 19. Resistance/Cycle graph of ITO 928-2 sample drawn with data obtained with 2-probe methods

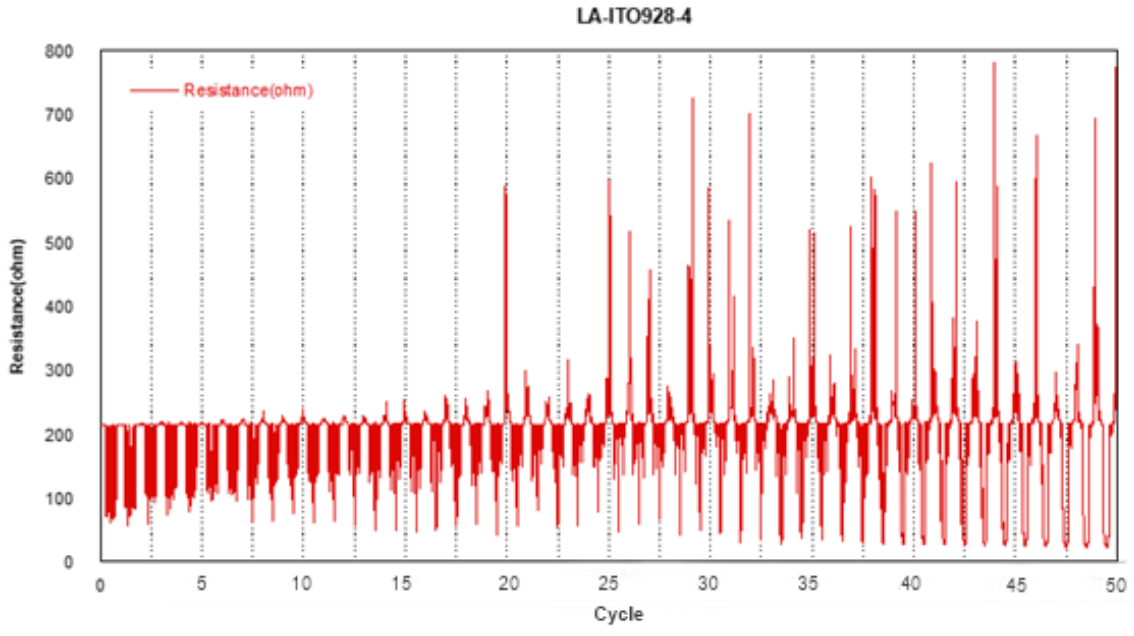

Figure 20. Resistance/Cycle graph of ITO 928-4 sample drawn with data obtained with 2-probe methods

When these graphs were examined in detail, a high amount of contact resistance was detected at the peaks. To obtain more precise measurements from these samples and eliminate the observed contact resistance, data were taken using the 4-probe method

during the bending cycle. The graphs drawn with these data are seen in Figure 21 and Figure 22**.** Figure 23 shows the comparative graph of two ITO samples**.**

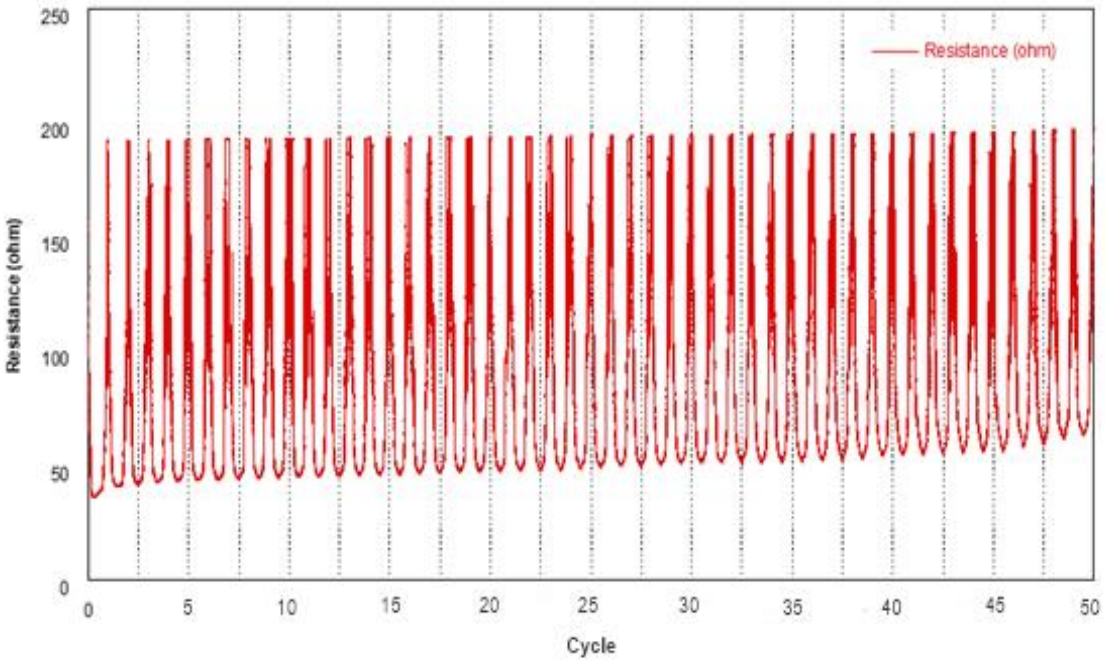

Figure 21. Resistance/Cycle graph of ITO 928-2 sample drawn with data obtained with 4-probe methods

When the changes between the peak and trough points of the graph for Figure 21 are examined, that is, when the changes between the maximum bending point and the initial state of the ITO coated sample are taken into consideration, an average difference of 140-150 Ωs is seen for each cycle. The image of the sample during the bending process is presented in Figure 11 and 12.

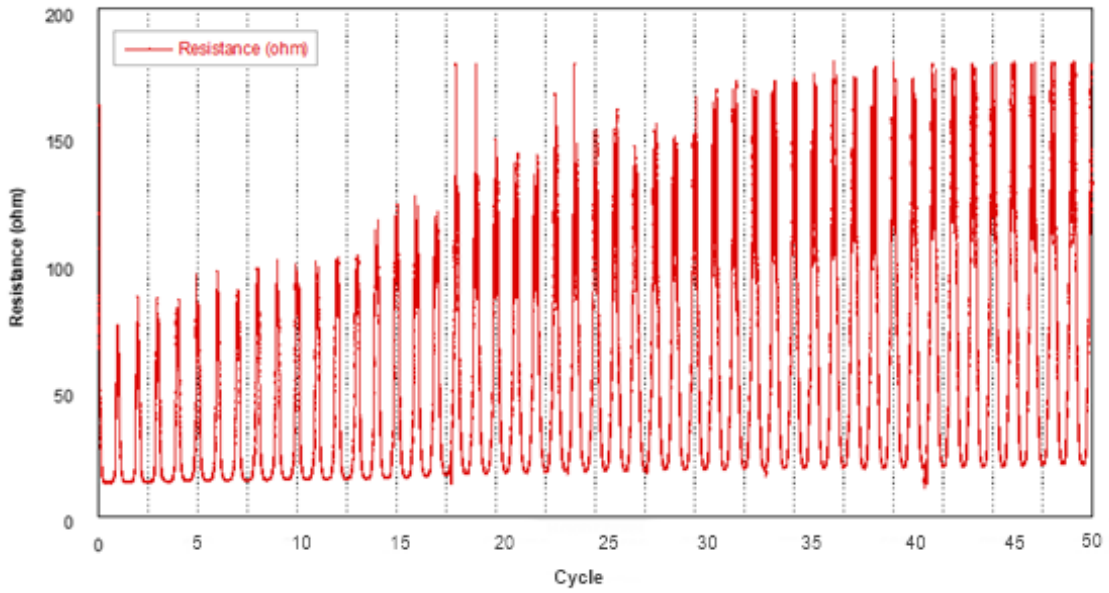

Figure 22. Resistance/Cycle graph of ITO 928-4 sample drawn with data obtained with 4-probe methods

When the changes between the same points are examined for Figure 22, it is determined that the average changes are between 150 Ωs and 20 Ωs and an average of 120-130 Ωs difference is seen for each cycle.

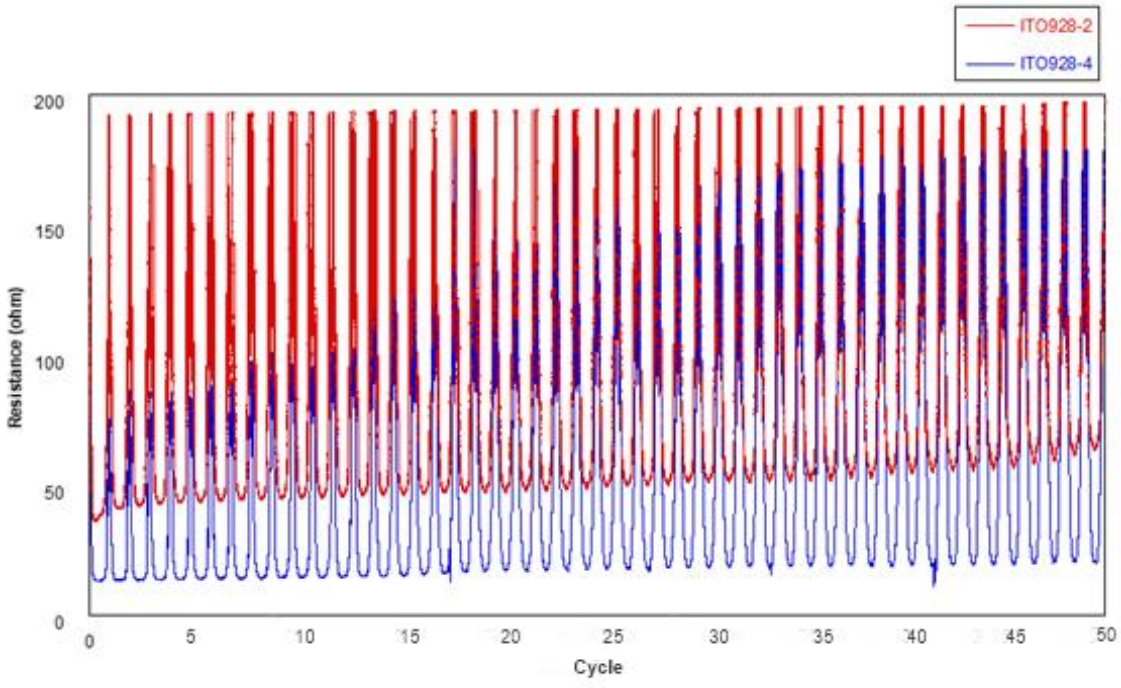

Figure 23. Resistance/Cycle comparison graph of ITO 928-2 and ITO 928-4 sample

In Figure 23, where the two samples are compared, it is noteworthy that similar results are obtained between the two samples as expected. As can be seen from this graph, the coatings on the substrates and the measurement results support each other.

The graphics of the ZAZ thin film coated samples are presented in Figure 24, Figure 25 and Figure 26.

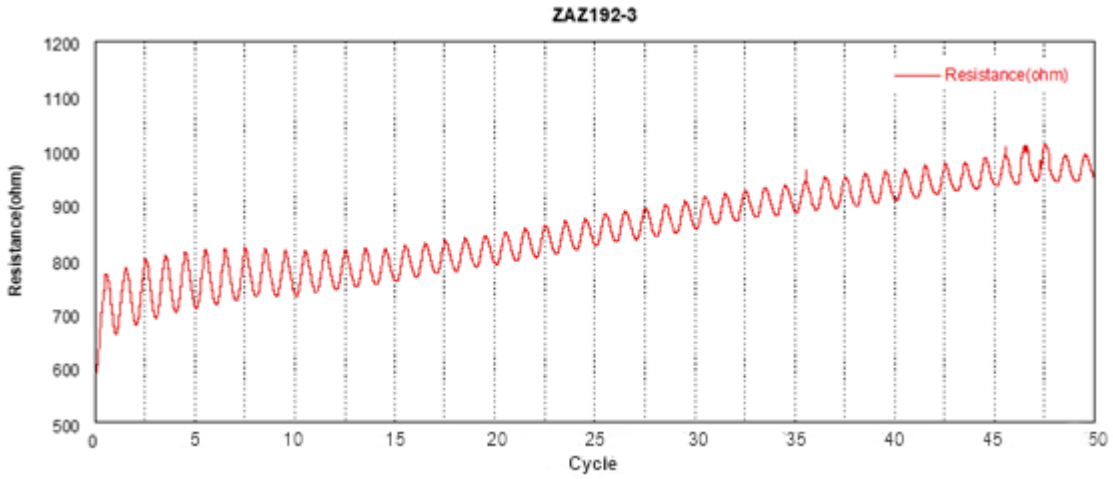

Figure 24. Resistance/Cycle graph of ZAZ 192-3 sample drawn with data obtained with 2-probe methods

The Resistance/Cycle graph of the ZAZ 192-3 sample is seen in Figure 24. When the graph resulting from the data taken for this sample is examined, it is seen that the average change between the peak and trough points is 60 Ωs.

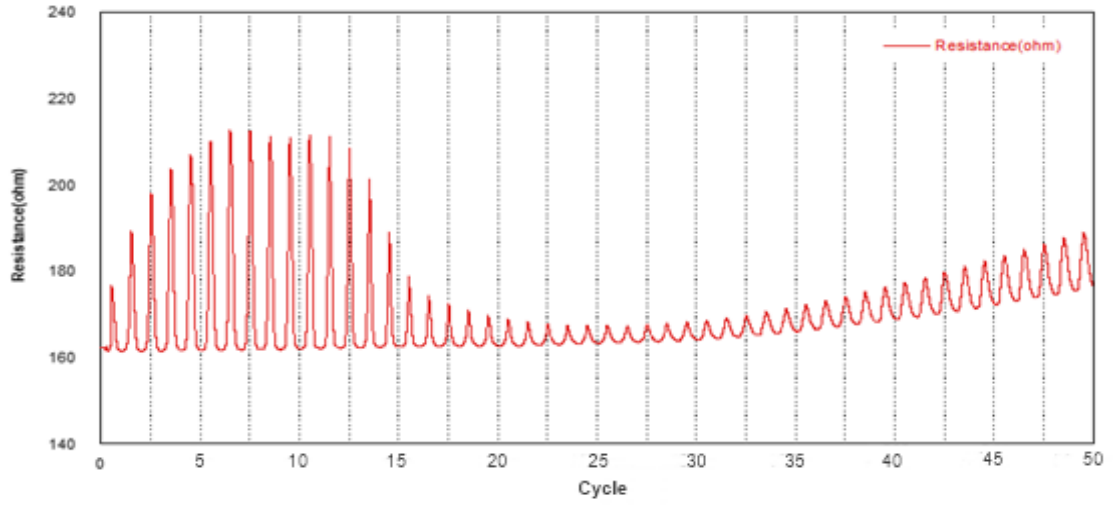

Figure 25. Resistance/Cycle graph of ZAZ 193-3 sample drawn with data obtained with 2-probe methods

When similar points are investigated in Figure 25, in this graph where differences of 10 Ωs are seen in places, the average change is in the range of 160-180 Ωs and this difference is determined as 20 Ωs on average.

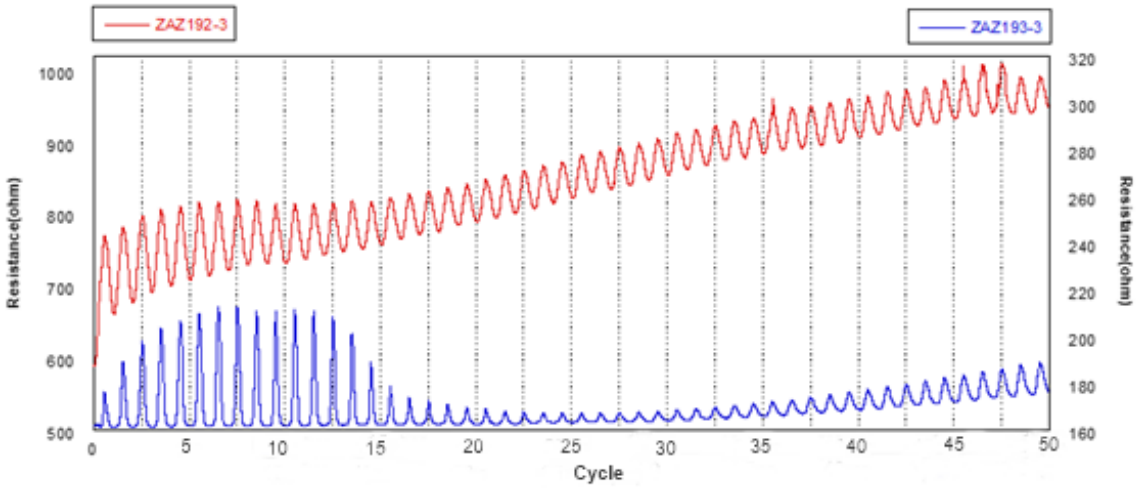

Figure 26. Resistance/Cycle comparison graph of ZAZ 192-3 and ZAZ 193-3 sample

In Figure 26, the Resistance/Cycle graphs of the ZAZ thin film coated samples are presented together. When Figure 26 and Figure 23 are compared with each other, it is seen that the graphs of the ZAZ samples are more consistent in shape than the graphs of the ITO coated samples.

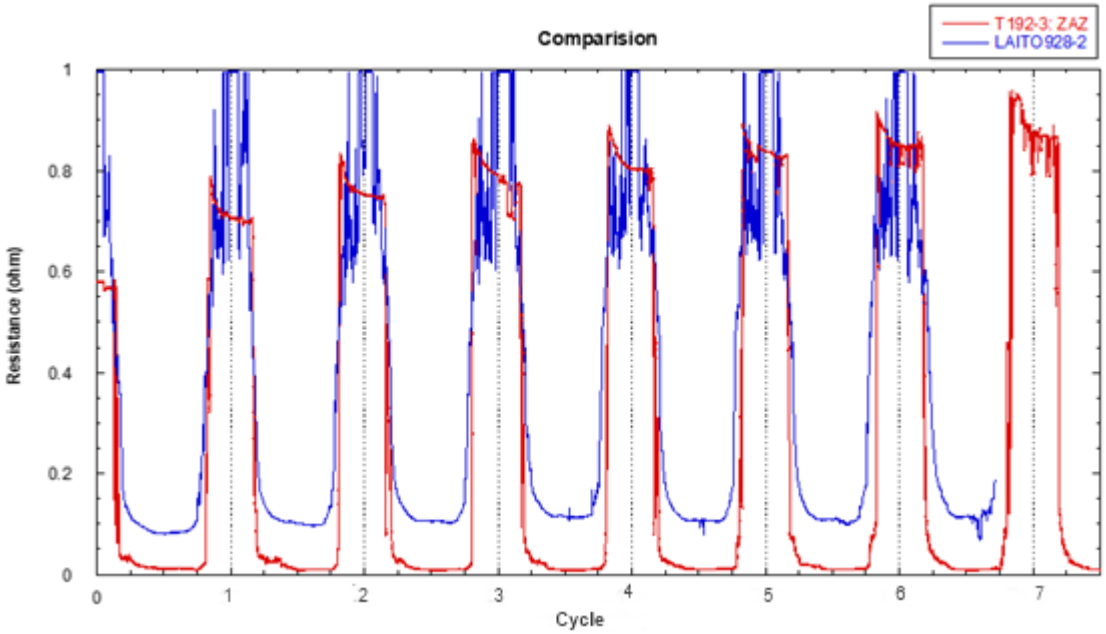

Figure 27. Comparative graph of normalized Resistance/Cycle of ZAZ192-3 and ITO 928-2 sample

In Figure 27, the resistance data up to approximately 7 cycles were normalized and plotted on figure for more detailed analysis of the ZAZ 192-3 and ITO 928-2 samples.

When the behaviors of the two samples at the peaks are investigated, it is clearly seen that the ZAZ coated sample shows a smooth change while the ITO coated rulers show irregular and unordered changes. The reason for these irregularities the cracks formed in the ITO thin films, as can be seen in the SEM analysis in the physical characterization section.

Due to the small change between the peak and trough points on the graph is the most important factor in terms of the applicability of a coating on flexible substrates. In the case of a significant difference, a decrease in electrical conductivity levels is expected. Furthermore, it is predicted that in the final product where the coating will be applied, non-repeating cycles may occur, leading to unpredictable behavior in the conductivity levels.

The results obtained when the electrical characterization is performed pave the way for the use of ZAZ thin film coatings for flexible optoelectronic devices and wearable materials.

4.3. Optical Characterization

For optical transmission, the transmission values of ITO and ZAZ thin film coated samples before and after the bending cycle, approximately 550 nm in the visible region range, were investigated.

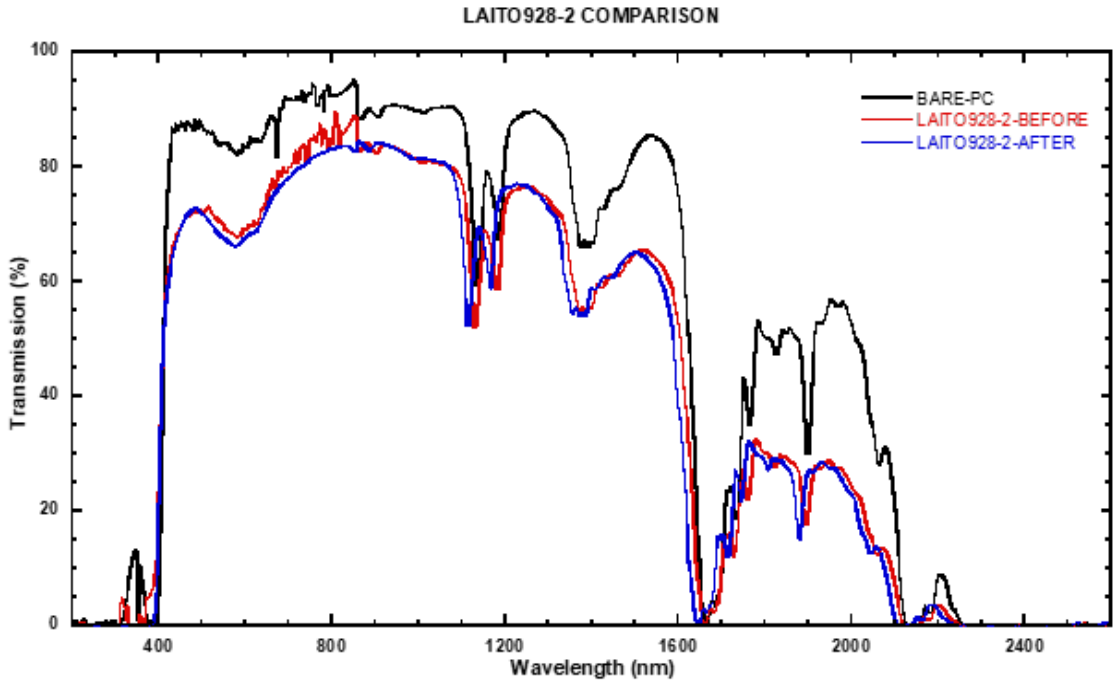

Figure 28. Transmission graphs of the ITO 928-2 sample before and after the bending cycle

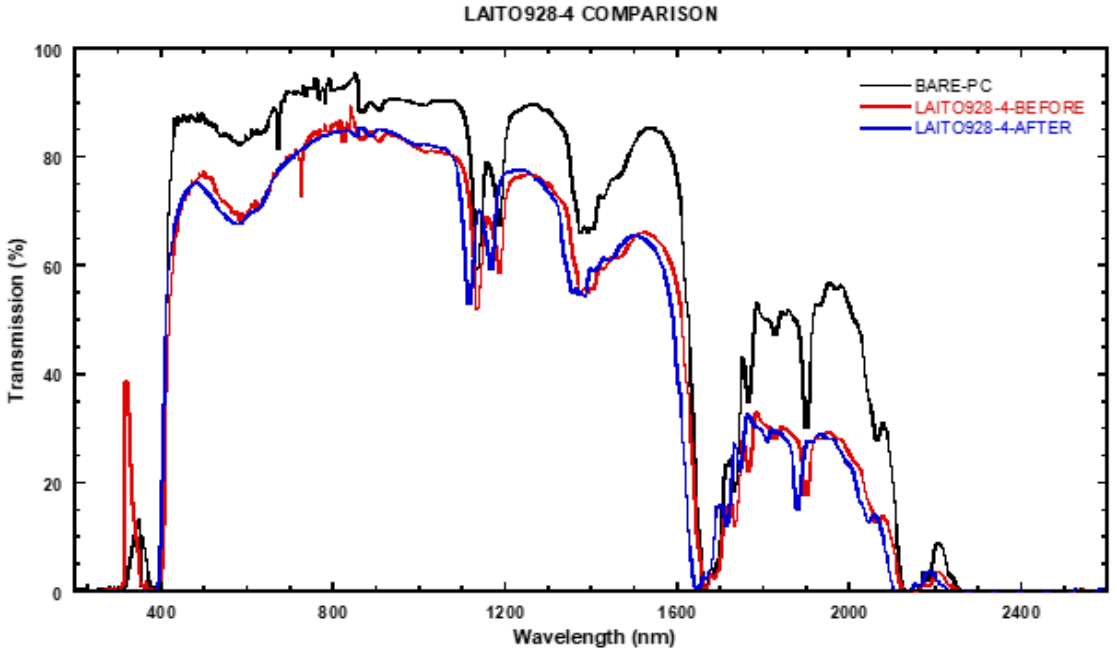

Figure 29. Transmission graphs of the ITO 928-4 sample before and after the bending cycle

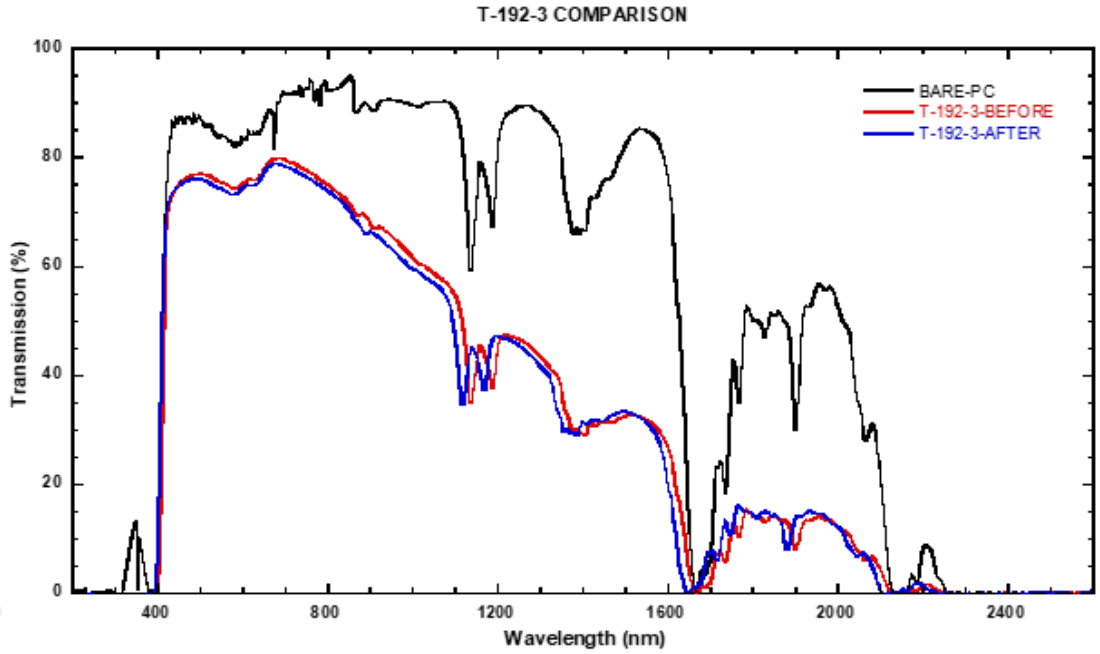

Figure 30. Transmission graphs of the ZAZ 192-3 sample before and after the bending cycle

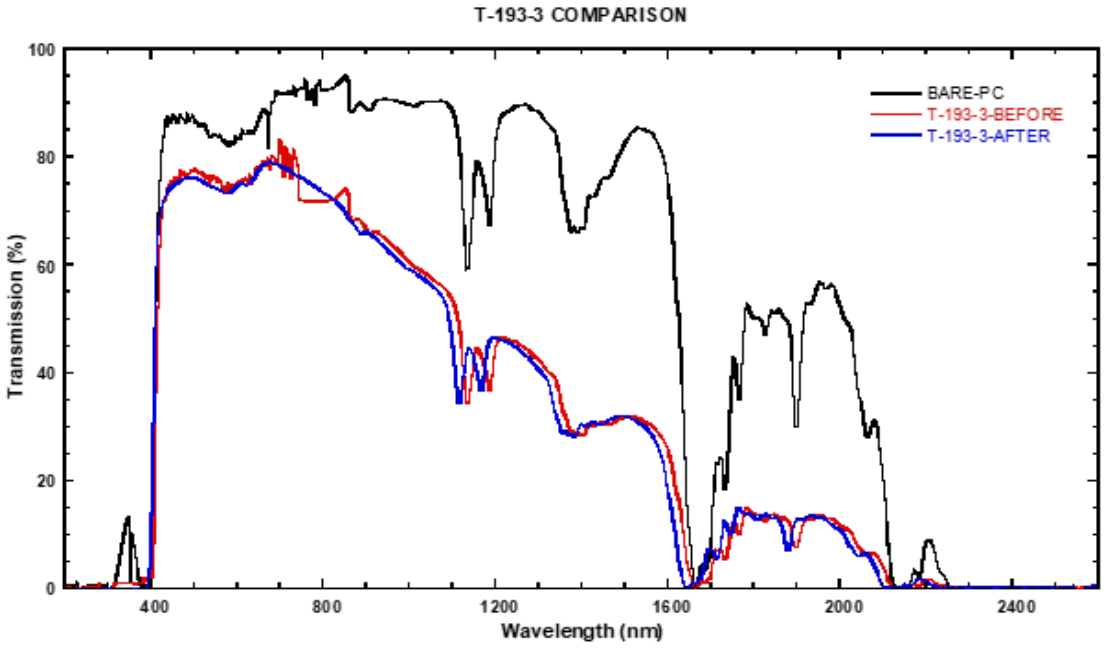

Figure 31. Transmission graphs of the ZAZ 193-3 sample before and after the bending cycle

In Figure 28, Figure 29, Figure 30 and Figure 31, the transmission values for ITO 928-2, ITO 929 4, ZAZ 192-3 and ZAZ 193-3 samples before and after the bending cycle are presented comparatively. As expected, as a result of the investigations,

a decrease of 1.95% for ITO 928-2 sample, 2.56% for ITO 928-3 sample, 1.18% for ZAZ 192-3 sample and 1.21% for ZAZ 193-3 sample was observed at approximately 550 nm. The obtained data is presented in Table 8. The transmission values of interest are at a wavelength of approximately 550 nm. The wavelength at which photons from the Sun are most intense is 550 nm and is located in the middle of the visible light spectrum. For this reason, it is in the region to which the human eye is most sensitive.

Table 8. Transmission values measured before and after the bending cycle

	Transmission (%) (~550 nm)		
Sample	**Before Bending**	**After Bending**	**Difference**
ITO 928-2	69.45 ± 0.73	67.50 ± 0.98	-1.95
ITO 928-4	71.68 ± 0.84	69.12 ± 0.92	-2.56
ZAZ 192-3	75.47 ± 0.42	74.29 ± 0.18	-1.18
ZAZ 193-3	75.50 ± 0.44	74.29 ± 0.26	-1.21

When the transmission values of the ITO coated ruler samples were compared with the values of the ZAZ coated samples, a decrease of approximately 2 times was observed. Although this change on the rulers is physically incomprehensible to the naked eye, it is an undeniable amount in the final product production.

Upon close examination of the transmission spectra, a significant decline in transmission values is observed in the wavelength range below 400 nm. This reduction can be attributed to the band gap properties of the substrate. The uniformity of this decline across all spectra within the region of interest suggests that it is primarily linked to the band gap energy of the substrate rather than that of the thin films. The PC material employed as the substrate exhibits strong absorption characteristics for wavelengths shorter than 400 nm, resulting in a transmission value that approaches zero in this region.

4.4. Electromagnetic Shielding

S21 transmission measurement was conducted operating in the frequency range of 8.20 GHz to 12.40 GHz with a WR90 waveguide, and the resulting data was used to draw S21 graphs against frequency.

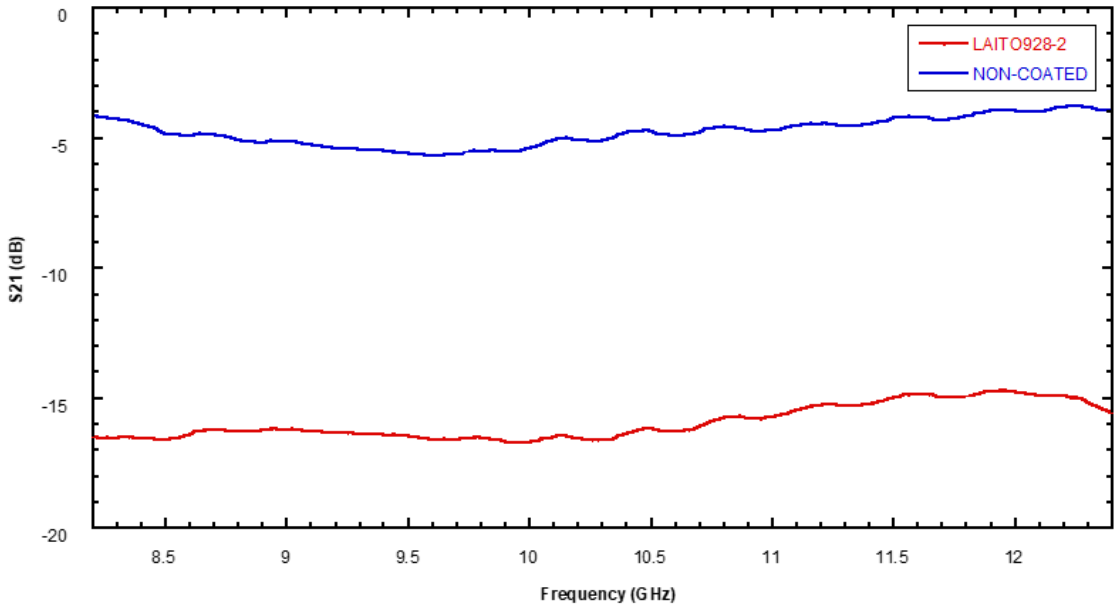

Figure 32. S21 Transmission graph of LAITO928-2 sample

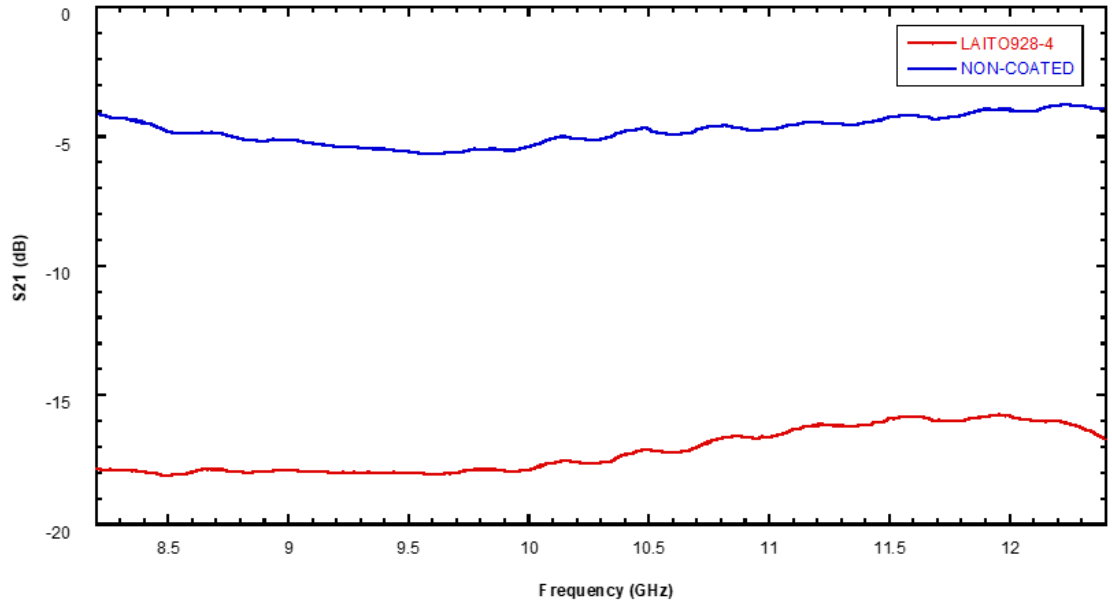

Figure 33. S21 Transmission graph of LAITO928-4 sample

Figure 32 and 33 the frequency-dependent S21 graphs for ITO samples are shown. In the measured frequency range, S21 values are observed to be around -16, -17 dB for the LAITO928-2 sample, while they are around -17, -18 dB for the LAITO 928-4 sample.

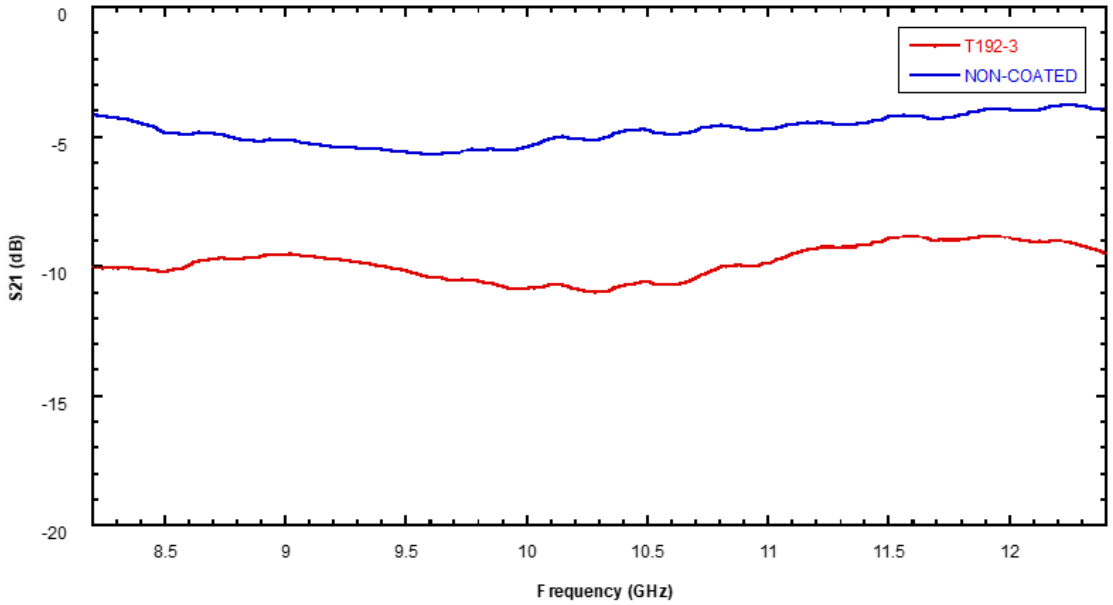

Figure 34. S21 Transmission graph of T192-3 sample

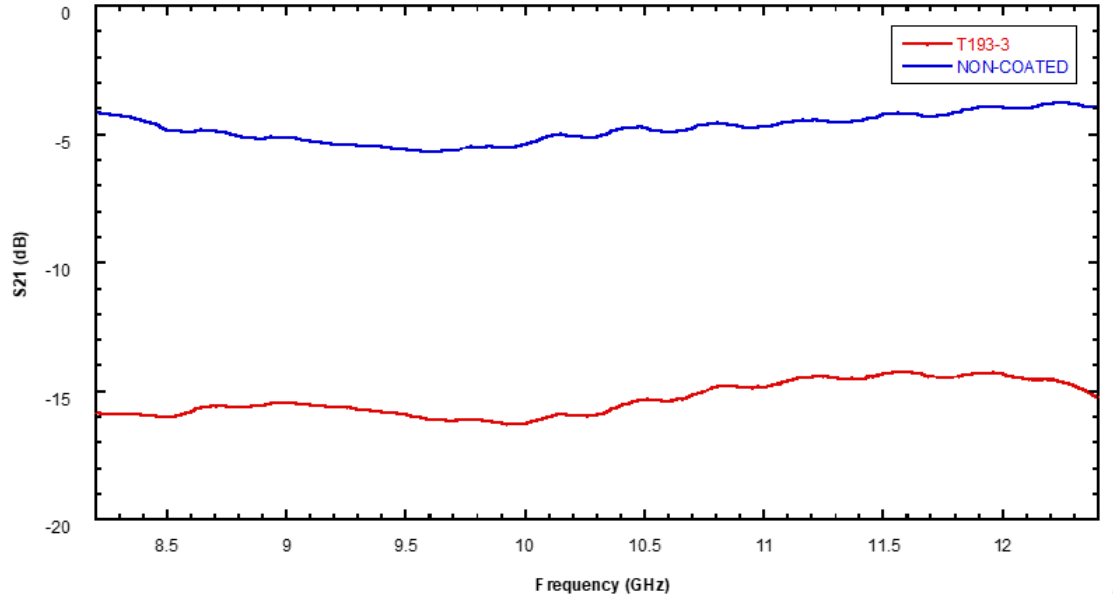

Figure 35. S21 Transmission graph of T193-3 sample

Figure 34 and 35 the frequency-dependent S21 graphs for ZAZ samples are shown. In the measured frequency range, S21 values are observed to be around -9, -11 dB for the T192-3 sample, while they are around -15, -16 dB for the T193-3 sample.

As mentioned under the heading 3.6.4., the decrease in the power ratio ratio, i.e. the negative increase in S21 values, shows that the attenuation value increases and therefore the transmission decreases. In line with this information, when the S21 values

of the ITO and ZAZ samples are compared, it is observed that the ZAZ samples give higher transmission in certain frequency ranges compared to ITO, which is frequently used in the literature.

CHAPTER 5

CONCLUSION

In this thesis, the studies commenced with the preparation of substrates, followed by the growth of thin films and subsequent characterization processes. Polycarbonate (PC) ruler substrates were fabricated by cutting large flexible polycarbonate sheets into dimensions of 30 x 3 x 0.6 cm. ZTO/Ag/ZTO (ZAZ) thin film coatings were applied to the prepared ruler samples using the DC magnetron sputtering technique, employing optimized parameters at room temperature within a cylindrical vacuum system featuring a diameter and length of 150 cm. Indium Tin Oxide (ITO) samples were prepared utilizing the same method under identical conditions in a mobile inline vacuum system. After the bending process was performed on the fabricated ZTO/Ag/ZTO and ITO thin film samples, their structural, optical, and electrical properties were characterized.

Within the optimized parameters, 80 sccm Ar and 2.5 sccm O_2 gas were sent to the vacuum system for ITO coatings. The target sample distance was set as 7.5 cm, DC power as 900w and sample holder speed as 9cm/min. 137 sccm Ar gas was sent to the vacuum chamber for ZTO, Ag and Au coatings. For the ZTO layer, the target sample distance was set to 8 cm, the DC power was set to an average of 77 W and the target speed was set to 10cm/min. For the Ag layer, the target sample distance was set to 10 cm, the DC power was set to an average of 48 W and the target speed was set to 80cm/min. Finally, for the Au contact layer required for electrical characterization, the target sample distance was set to 7cm, the DC power was set to an average of 45 W and the target speed was set to 9cm/min.

In the structural characterization of the films, the adhesion strength of the films was first examined. In order to evaluate the performance of the films on the substrates, the tape test method was used, in which the remaining film amount and surface condition were observed by placing tape on them and then removing them. When the results were evaluated, it was seen that the films did not separate from the surface and did not show any signs of breakage when the tape was removed; this shows that both films showed high adhesion quality and strength.

As a result of the thickness measurements of the samples, the thickness of the ITO coatings was determined as 247 nm and the thickness of the ZAZ coatings as 34 nm/15 nm/35 nm, respectively. The thickness of the gold layer, which is the contact layer, was measured as 69 nm. At these thickness values, the maximum conductivity and maximum optical transparency data were achieved in ZAZ and ITO thin films in accordance with the literature research.

SEM analysis after 50 bending cycles reveal that ZAZ-coated samples exhibited fewer cracks compared to ITO-coated samples, indicating better structural integrity. CBS-Z Contrast imaging of ITO samples further showed that cracks corresponded to low atomic number carbon atoms, while the brighter areas represented high atomic number indium atoms. The increased cracking in ITO samples explains the irregularities observed in the normalized cycle-dependent resistance graph of Figure 27, suggesting that ZAZ coatings offer superior mechanical flexibility and durability under stress.

For the electrical characterization of the samples, the behavior during the bending cycle process was recorded. The 2-probe method was used for the ZAZ samples and the 4-probe method was used for the ITO samples. These methods are detailed under the title Electrical Characterization. When the change between the maximum bending point of the 2nd sample with ITO coating during the bending process and the initial state was examined, it was seen that it was 140-150 Ωs and 120-130 Ωs for the 4th sample. When the ZAZ coated samples were examined under the same conditions, it was seen that this change was 60 Ωs and 10 Ωs on average. The high resistance change during the bending process will both reduce the electrical conductivity and create an undesirable situation that will prevent balanced and stable electrical transfer. The irregular changes that occur at the peaks of the ITO coating in the detailed graph seen in Figure 27 prove the cracks that occur in the ITO coating at the end of the bending process.

When the optical characterization of the samples was performed, the difference between the transmission values before and after the bending process was applied at approximately 550 nm was 1.95% - 2.56% in ITO coated samples 928-2 and 928-4, and 1.18% - 1.21% in ZAZ coated samples 192-3 and 193-3. When these difference values were compared, a change of approximately 2-fold supported the use of ZAZ coating as an alternative to ITO coatings. A significant decline in transmission values below 400 nm is observed, attributed to the band gap properties of the substrate rather than the thin films. The polycarbonate substrate absorbs light in this wavelength range, resulting in transmission approaching zero.

Finally, when the samples were subjected to Electromagnetic Shielding Measurements, S21 measurements revealed that ZAZ samples exhibit higher transmission than ITO samples. While ITO (LAITO928-2 and LAITO928-4) shows S21 values ranging from -16 to -18 dB, ZAZ (T192-3 and T193-3) ranges from -9 to -16 dB, indicating better performance. The observed decrease in power ratio confirms that increased attenuation leads to decreased transmission. This suggests that ZAZ materials may be advantageous for applications needing higher transmission.

The characterizations made in this thesis study show that ZAZ coatings can offer higher performance or cost advantages. As a result, due to their excellent electrical and optical properties, ZTO/Ag/ZTO thin films offer a promising option for TCO applications compared to ITO thin films. This study provides a strong basis for investigating the suitability of flexible TCOs for applications requiring mechanical flexibility and for developing innovative flexible optoelectronic devices.

REFERENCES

Armouzi, Naoual Al, Mohamed Manoua, Ghizlan El Hallani, Hikmat S. Hilal, Ahmed Liba, Nourreeddine Kouider, and Mustapha Mabrouki. 2021. "Effects of Sn Doping on Properties of Multilayered ZnO Films Deposited by Spin Coating/Sol–Gel Method." *JOM* 73 (1): 411–19. https://doi.org/10.1007/s11837-020-04492-y.

Baxter, Jason B., and Eray S. Aydil. 2006. "Dye-Sensitized Solar Cells Based on Semiconductor Morphologies with ZnO Nanowires." *Solar Energy Materials and Solar Cells* 90 (5): 607–22. https://doi.org/10.1016/j.solmat.2005.05.010.

Badeker, K. 1907. "Concerning the Electricity Conductivity and Thermoelectric Energy of Several Heavy Metal Bonds." *Annalen der Physik*, 327(4), 749-766. https://doi.org/10.1002/andp.19073270409

Behrendt, Andreas, Christian Friedenberger, Tobias Gahlmann, Sara Trost, Tim Becker, Kirill Zilberberg, Andreas Polywka, Patrick Görrn, and Thomas Riedl. 2015. "Highly Robust Transparent and Conductive Gas Diffusion Barriers Based on Tin Oxide." *Advanced Materials* 27 (39): 5961–67. https://doi.org/10.1002/adma.201502973.

Betz, U., M. Kharrazi Olsson, J. Marthy, M. F. Escolá, and F. Atamny. 2006. "Thin Films Engineering of Indium Tin Oxide: Large Area Flat Panel Displays Application." *Surface and Coatings Technology* 200 (20–21): 5751–59. https://doi.org/10.1016/j.surfcoat.2005.08.144.

Bingel, Astrid, Olaf Stenzel, Philipp Naujok, Robert Müller, Svetlana Shestaeva, Martin Steglich, Ulrike Schulz, Norbert Kaiser, and Andreas Tünnermann. 2016. "AZO/Ag/AZO Transparent Conductive Films: Correlation between the Structural, Electrical, and Optical Properties and Development of an Optical Model." *Optical Materials Express* 6 (10): 3217. https://doi.org/10.1364/ome.6.003217.

Chiu, Po-Kai, Chao-Te Lee, Donyau Chiang, Wen-Hao Cho, Chien-Nan Hsiao, Yi-Yan Chen, Bo-Ming Huang, and Jer-Ren Yang. 2014. "Conductive and Transparent

Multilayer Films for Low-Temperature TiO 2 /Ag/SiO 2 Electrodes by E-Beam Evaporation with IAD." http://www.nanoscalereslett.com/content/9/1/35.

Choi, Yoon Young, Kwang Hyuk Choi, Hosun Lee, Hosuk Lee, Jae Wook Kang, and Han Ki Kim. 2011. "Nano-Sized Ag-Inserted Amorphous ZnSnO3 Multilayer Electrodes for Cost-Efficient Inverted Organic Solar Cells." *Solar Energy Materials and Solar Cells* 95 (7): 1615–23. https://doi.org/10.1016/j.solmat.2011.01.013.

Chopra, K L, S Major, and D K Pandya. 1983. "Review Paper Transparent Conductors-a Status Review." *Electronics and Optics*. Vol. 102.

Dazai, Takuro, Shintaro Yasui, Tomoyasu Taniyama, and Mitsuru Itoh. 2020. "Bandgap Tuning and Optimization of Green-Emitting Zn2SnO4-Mg2SnO4:Mn2+ Using Combinatorial Pulsed Laser Deposition." *Ceramics International* 46 (13): 21771–74. https://doi.org/10.1016/j.ceramint.2020.05.288.

Dhamodharan, P., C. Manoharan, S. Dhanapandian, M. Bououdina, and S. Ramalingam. 2015. "Preparation and Characterization of Spray Deposited Sn-Doped ZnO Thin Films onto ITO Subtracts as Photoanode in Dye Sensitized Solar Cell." *Journal of Materials Science: Materials in Electronics* 26 (7): 4830–39. https://doi.org/10.1007/s10854-015-2990-7.

Ekmekcioglu, Merve, Nursev Erdogan, Aziz Taner Astarlioglu, Serap Yigen, Gulnur Aygun, Lutfi Ozyuzer, and Mehtap Ozdemir. 2021. "High Transparent, Low Surface Resistance ZTO/Ag/ZTO Multilayer Thin Film Electrodes on Glass and Polymer Substrates." *Vacuum* 187 (May). https://doi.org/10.1016/j.vacuum.2021.110100.

Ekmekçioğlu, MSc Thesis. 2019. "Growth and Characterization of ZnSnO Thin Films on Polymers for Oleds."

Ghorbani, Mohammad Matboo, and Reza Taherian. 2018. "Methods of Measuring Electrical Properties of Material." In *Electrical Conductivity in Polymer-Based Composites: Experiments, Modelling, and Applications*, 365–94. Elsevier. https://doi.org/10.1016/B978-0-12-812541-0.00012-4.

Ginley. 2011. “Handbook of Transparent Conductors.” *Springer US*. https://doi.org/10.1007/978-1-4419-1638-9.

Girtan, Mihaela. 2012. “Comparison of ITO/Metal/ITO and ZnO/Metal/ZnO Characteristics as Transparent Electrodes for Third Generation Solar Cells.” *Solar Energy Materials and Solar Cells* 100 (May):153–61. https://doi.org/10.1016/j.solmat.2012.01.007.

Granqvist, Claes G. 2007. “Transparent Conductors as Solar Energy Materials: A Panoramic Review.” *Solar Energy Materials and Solar Cells*. https://doi.org/10.1016/j.solmat.2007.04.031.

Guillén, C., and J. Herrero. 2011. “TCO/Metal/TCO Structures for Energy and Flexible Electronics.” *Thin Solid Films*. https://doi.org/10.1016/j.tsf.2011.06.091.

Hassan, Mohammad M. 2017. “Antimicrobial Coatings for Textiles.” In *Handbook of Antimicrobial Coatings*, 321–55. Elsevier. https://doi.org/10.1016/B978-0-12-811982-2.00016-0.

Hengst, Claudia, Siegfried B. Menzel, Gayatri K. Rane, Vladimir Smirnov, Karen Wilken, Barbara Leszczynska, Dustin Fischer, and Nicole Prager. 2017. “Mechanical Properties of ZTO, ITO, and a-Si: H Multilayer Films for Flexible Thin Film Solar Cells.” *Materials* 10 (3). https://doi.org/10.3390/ma10030245.

Heo, Y. W., Y. W. Kwon, Y. Li, S. J. Pearton, and D. P. Norton. 2004. “P-Type Behavior in Phosphorus-Doped (Zn,Mg)O Device Structures.” *Applied Physics Letters* 84 (18): 3474–76. https://doi.org/10.1063/1.1737795.

Hosono, Hideo. 2007. “Recent Progress in Transparent Oxide Semiconductors: Materials and Device Application.” *Thin Solid Films* 515 (15 SPEC. ISS.): 6000–6014. https://doi.org/10.1016/j.tsf.2006.12.125.

Jeong, Eunwook, Taehyeong Lee, Sang Geul Lee, Seung Min Yu, Jong Seong Bae, Gun Hwan Lee, Dooho Choi, and Jungheum Yun. 2021. “Thermal Stability Enhancement of Ultrathin Ag Film Electrodes by Incorporating Atomic Oxygen.” *Applied Surface Science* 546 (April). https://doi.org/10.1016/j.apsusc.2021.149149.

Jeong, Jin A., Yong Seok Park, and Han Ki Kim. 2010. “Comparison of Electrical, Optical, Structural, and Interface Properties of IZO-Ag-IZO and IZO-Au-IZO Multilayer Electrodes for Organic Photovoltaics.” *Journal of Applied Physics* 107 (2). https://doi.org/10.1063/1.3294605.

Jung, Yu Sup, Yong Seo Park, Kyung Hwan Kim, and Won Jae Lee. 2013. “Properties of AZO/Ag/AZO Multilayer Thin Film Deposited on Polyethersulfone Substrate.” *Transactions on Electrical and Electronic Materials* 14 (1): 9–11. https://doi.org/10.4313/TEEM.2013.14.1.9.

Kao, Yu Han, Hung Shuo Chang, and Chiao Chi Lin. 2023. “Reliability Analysis of Laminated Oxide/Metal/Oxide Flexible Conductors Through Cyclic Bending after Accelerated Weathering.” In *IFETC 2023 - 5th IEEE International Flexible Electronics Technology Conference, Proceedings*. Institute of Electrical and Electronics Engineers Inc. https://doi.org/10.1109/IFETC57334.2023.10254833.

Kao, Yu Han, Hung Shuo Chang, Chih Chieh Wang, and Chiao Chi Lin. 2022. “Weathering and Material Characterization of ZTO/Ag/ZTO Coatings on Polyethylene Terephthalate Substrates for the Application of Flexible Transparent Conductors.” *Coatings* 12 (9). https://doi.org/10.3390/coatings12091249.

Katayama, M. 1999. “TFT-LCD Technology.” *Thin Solid Films* 341(1-2), 140-147. https://doi.org/10.1016/S0040-6090(98)01519-3

Kim, Dae Hyun, Han Kyeol Lee, Jin Young Na, Sun Kyung Kim, Young Zo Yoo, and Tae Yeon Seong. 2015. “ZnSnO/Ag/Indium Tin Oxide Multilayer Films as a Flexible and Transparent Electrode for Photonic Devices.” *Superlattices and Microstructures* 83 (July):635–41. https://doi.org/10.1016/j.spmi.2015.04.002.

Lewis, B.G., Paine, D.C. 2000. “Applications and Processing of Transparent Conducting Oxides Large-Scale Manufacturing of ITO Thin-Film Coatings.”

Lim, Jong Wook, Se In Oh, Kyoungtae Eun, Sung Hoon Choa, Hyun Woo Koo, Tae Woong Kim, and Han Ki Kim. 2012. “Mechanical Flexibility of ZnSnO/Ag/ZnSnO Films Grown by Roll-to-Roll Sputtering for Flexible Organic Photovoltaics.” *Japanese Journal of Applied Physics* 51 (11). https://doi.org/10.1143/JJAP.51.115801.

Martin, E. J.J., M. Yan, M. Lane, J. Ireland, C. R. Kannewurf, and R. P.H. Chang. 2004. "Properties of Multilayer Transparent Conducting Oxide Films." *Thin Solid Films* 461 (2): 309–15. https://doi.org/10.1016/j.tsf.2004.01.103.

Mirletz, Heather M., Kelly A. Peterson, Ina T. Martin, and Roger H. French. 2015. "Degradation of Transparent Conductive Oxides: Interfacial Engineering and Mechanistic Insights." *Solar Energy Materials and Solar Cells* 143 (August):529–38. https://doi.org/10.1016/j.solmat.2015.07.030.

Mohamed, S. H. 2008. "Effects of Ag Layer and ZnO Top Layer Thicknesses on the Physical Properties of ZnO/Ag/Zno Multilayer System." *Journal of Physics and Chemistry of Solids* 69 (10): 2378–84. https://doi.org/10.1016/j.jpcs.2008.03.019.

Mylvaganam, Kausala, Yiqing Chen, Weidong Liu, Mei Liu, and Liangchi Zhang. 2014. "Hard Thin Films: Applications and Challenges." In *Anti-Abrasive Nanocoatings: Current and Future Applications*, 544–67. Elsevier Inc. https://doi.org/10.1016/B978-0-85709-211-3.00021-2.

Ozbay, Salih, Nursev Erdogan, Fuat Erden, Merve Ekmekcioglu, Mehtap Ozdemir, Gulnur Aygun, and Lutfi Ozyuzer. 2020. "Surface Free Energy Analysis of ITO/Au/ITO Multilayer Thin Films on Polycarbonate Substrate by Apparent Contact Angle Measurements." *Applied Surface Science* 529 (November). https://doi.org/10.1016/j.apsusc.2020.147111.

Park, Jun Hyuk, Han Ki Kim, Hosuk Lee, Hosun Lee, Sooyoung Yoon, and Chang Dong Kim. 2010. "Highly Transparent, Low Resistance, and Cost-Efficient Nb: TiO 2/Ag/Nb: TiO2 Multilayer Electrode Prepared at Room Temperature Using Black Nb: TiO2 Target." *Electrochemical and Solid-State Letters* 13 (5). https://doi.org/10.1149/1.3313361.

Pasquarelli, Robert M., David S. Ginley, and Ryan O'hayre. 2011. "Solution Processing of Transparent Conductors: From Flask to Film." *Chemical Society Reviews* 40 (11): 5406–41. https://doi.org/10.1039/c1cs15065k.

Ruske, F., C. Jacobs, V. Sittinger, B. Szyszka, and W. Werner. 2007. "Large Area ZnO:Al Films with Tailored Light Scattering Properties for Photovoltaic

Applications." *Thin Solid Films* 515 (24 SPEC. ISS.): 8695–98. https://doi.org/10.1016/j.tsf.2007.03.107.

Sahu, D. R., Shin Yuan Lin, and Jow Lay Huang. 2006. "ZnO/Ag/ZnO Multilayer Films for the Application of a Very Low Resistance Transparent Electrode." *Applied Surface Science* 252 (20): 7509–14. https://doi.org/10.1016/j.apsusc.2005.09.021.

Sarma, Bikash, and Bimal K. Sarma. 2018. "Role of Residual Stress and Texture of ZnO Nanocrystals on Electro-Optical Properties of ZnO/Ag/ZnO Multilayer Transparent Conductors." *Journal of Alloys and Compounds* 734 (February):210–19. https://doi.org/10.1016/j.jallcom.2017.11.028.

Seok, Hae Jun, Hyeon Woo Jang, Dong Yeop Lee, Beom Gwon Son, and Han Ki Kim. 2019. "Roll-to-Roll Sputtered, Indium-Free ZnSnO/AgPdCu/ZnSnO Multi-Stacked Electrodes for High Performance Flexible Thin-Film Heaters and Heat-Shielding Films." *Journal of Alloys and Compounds* 775 (February):853–64. https://doi.org/10.1016/j.jallcom.2018.10.194.

Silva, Carlos, Jonas Deuermeier, Weidong Zhang, Emanuel Carlos, Pedro Barquinha, Rodrigo Martins, and Asal Kiazadeh. 2023. "Perspective: Zinc-Tin Oxide Based Memristors for Sustainable and Flexible In-Memory Computing Edge Devices." *Advanced Electronic Materials* 9 (11). https://doi.org/10.1002/aelm.202300286.

Singh, Anil, Sujeet Chaudhary, and D. K. Pandya. 2016. "High Conductivity Indium Doped ZnO Films by Metal Target Reactive Co-Sputtering." *Acta Materialia* 111 (June):1–9. https://doi.org/10.1016/j.actamat.2016.03.012.

Song, Jun Hyuk, Joon Woo Jeon, Yong Hyun Kim, Joon Ho Oh, and Tae Yeon Seong. 2013. "Optical, Electrical, and Structural Properties of ZrON/Ag/ZrON Multilayer Transparent Conductor for Organic Photovoltaics Application." *Superlattices and Microstructures* 62:119–27. https://doi.org/10.1016/j.spmi.2013.07.009.

Sumarni Mansur, Muhammad Nidzhom Zainol Abidin. 2024. "Sputtering Technique." *Advanced Ceramics for Photocatalytic Membranes*, 77–99.

Sutthana, S., N. Hongsith, and S. Choopun. 2010. "AZO/Ag/AZO Multilayer Films Prepared by DC Magnetron Sputtering for Dye-Sensitized Solar

Cell Application." *Current Applied Physics* 10 (3): 813–16. https://doi.org/10.1016/j.cap.2009.09.020.

Turkoglu, F., H. Koseoglu, M. Ekmekcioglu, A. Cantas, M. Ozdemir, G. Aygun, and L. Ozyuzer. 2022. "Development of ZTO/Ag/ZTO Transparent Electrodes for Thin Film Solar Cells." *Journal of Materials Science: Materials in Electronics* 33 (14): 10955–64. https://doi.org/10.1007/s10854-022-08075-2.

Turkoglu, F., H. Koseoglu, S. Zeybek, M. Ozdemir, G. Aygun, and L. Ozyuzer. 2018. "Effect of Substrate Rotation Speed and Off-Center Deposition on the Structural, Optical, and Electrical Properties of AZO Thin Films Fabricated by DC Magnetron Sputtering." *Journal of Applied Physics* 123 (16). https://doi.org/10.1063/1.5012883.

Tvarozek, Vladimir, Tibor Hianik, Ivan Novotny, Vlastimil Rehacek, Waldemar Ziegler, Rastislav Ivanic, and Marek Andel. 1998. "Thin Films in Biosensors." *Vacuum* 50 (3–4): 251–62. https://doi.org/10.1016/S0042-207X(98)00050-5.

Ukoba, K. O., A. C. Eloka-Eboka, and F. L. Inambao. 2018. "Review of Nanostructured NiO Thin Film Deposition Using the Spray Pyrolysis Technique." *Renewable and Sustainable Energy Reviews* 82 2900-2915. https://doi.org/10.1016/j.rser.2017.10.041

Winkler, Thomas, Hans Schmidt, Harald Flügge, Fabian Nikolayzik, Ihno Baumann, Stephan Schmale, Hans Hermann Johannes, et al. 2012. "Realization of Ultrathin Silver Layers in Highly Conductive and Transparent Zinc Tin Oxide/Silver/Zinc Tin Oxide Multilayer Electrodes Deposited at Room Temperature for Transparent Organic Devices." In *Thin Solid Films*, 520:4669–73. https://doi.org/10.1016/j.tsf.2011.10.122.

Wu, Chu Chun, Pang Shiu Chen, Cheng Hsiung Peng, and Ching Chiun Wang. 2013. "TiOx/Ag/TiOx Multilayer for Application as a Transparent Conductive Electrode and Heat Mirror." *Journal of Materials Science: Materials in Electronics* 24 (7): 2461–68. https://doi.org/10.1007/s10854-013-1118-1.

Yu, Shihui, Weifeng Zhang, Lingxia Li, Dan Xu, Helei Dong, and Yuxin Jin. 2014. "Optimization of SnO2/Ag/SnO2 Tri-Layer Films as Transparent Composite

Electrode with High Figure of Merit." *Thin Solid Films* 552 (February):150–54. https://doi.org/10.1016/j.tsf.2013.11.109.

Yu, Shijin, Wanmei Xu, Hua Zhu, Wangren Qiu, Qiuyun Fu, and Lingbing Kong. 2021. "Effect of Sputtering Power on Structure and Properties of ZTO Films." *Journal of Alloys and Compounds* 883 (November). https://doi.org/10.1016/j.jallcom.2021.160622.

Yu, Zhinong, Jian Leng, Wei Xue, Ting Zhang, Yurong Jiang, Jie Zhang, and Dongpu Zhang. 2012. "Highly Flexible Transparent and Conductive ZnS/Ag/ZnS Multilayer Films Prepared by Ion Beam Assisted Deposition." *Applied Surface Science* 258 (7): 2270–74. https://doi.org/10.1016/j.apsusc.2011.09.099.

Zhang, Yong Hui, Zeng Xia Mei, Hui Li Liang, and Xiao Long Du. 2017. "Review of Flexible and Transparent Thin-Film Transistors Based on Zinc Oxide and Related Materials." *Chinese Physics B*. Institute of Physics Publishing. https://doi.org/10.1088/1674-1056/26/4/047307.

Zhu, Hua, Hemei Wang, Wenqiong Wan, Shijin Yu, and Xiaowei Feng. 2014. "Influence of Oxygen and Argon Flow on Properties of Aluminum-Doped Zinc Oxide Thin Films Prepared by Magnetron Sputtering." *Thin Solid Films* 566 (September):32–37. https://doi.org/10.1016/j.tsf.2014.07.021.

Zhu, Hua, Hai Zhang, Tian hao Zhang, Shi jin Yu, Ping chun Guo, Yan xiang Wang, and Zhi sheng Yang. 2021. "Optical and Electrical Properties of ITO Film on Flexible Fluorphlogopite Substrate." *Ceramics International* 47 (12): 16980–85. https://doi.org/10.1016/j.ceramint.2021.02.269.

Zhu, Yanwu, Hendry Izaac Elim, Yong Lim Foo, Ting Yu, Yanjiao Liu, Wei Ji, Jim Yang Lee, et al. 2006. "Multiwalled Carbon Nanotubes Beaded with ZnO Nanoparticles for Ultrafast Nonlinear Optical Switching." *Advanced Materials* 18 (5): 587–92. https://doi.org/10.1002/adma.200501918.